Naval Research Reviews

Office of Naval Research
Two / 1996
Vol XLVIII

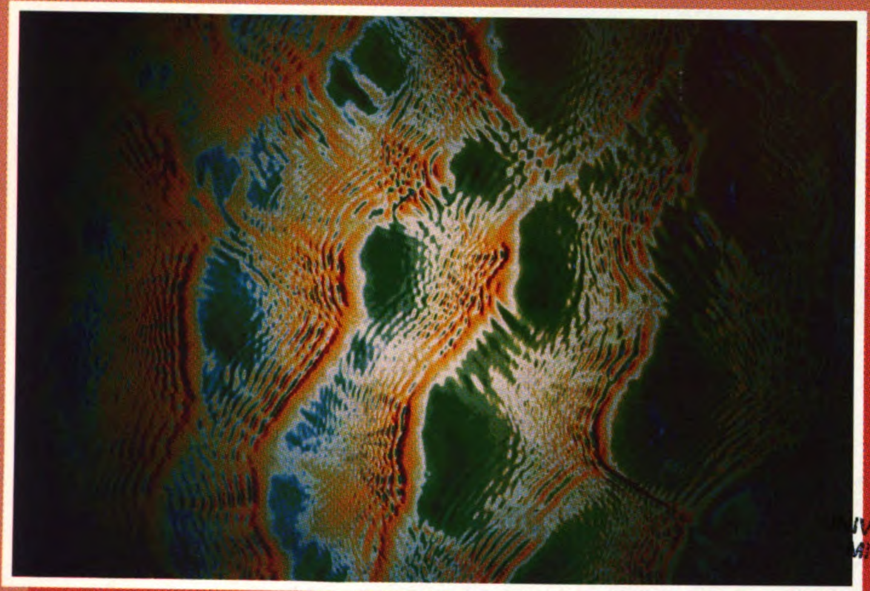

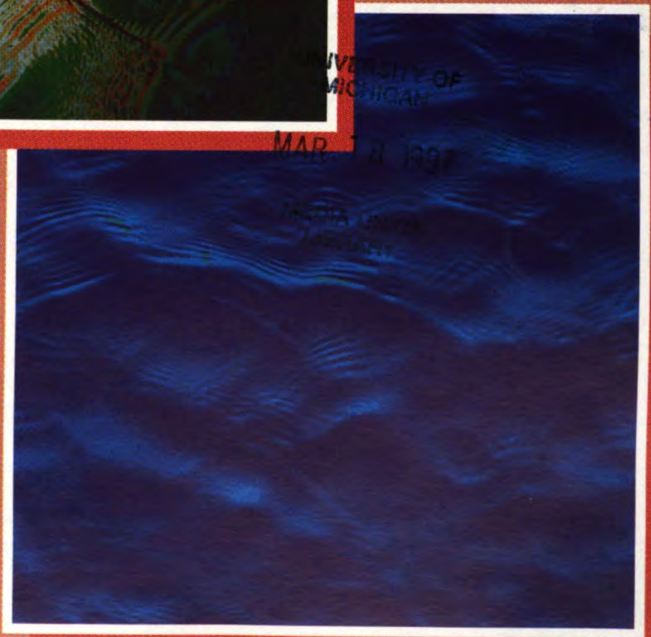

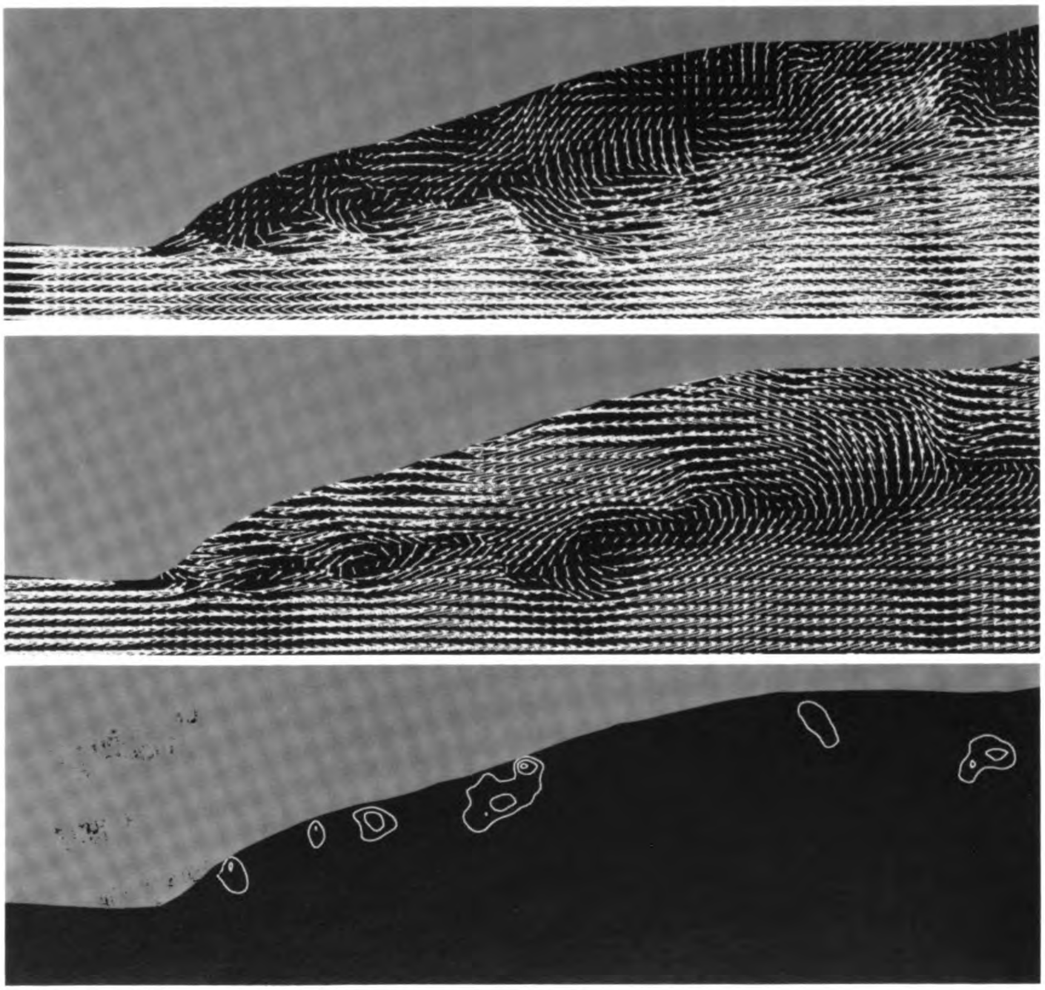

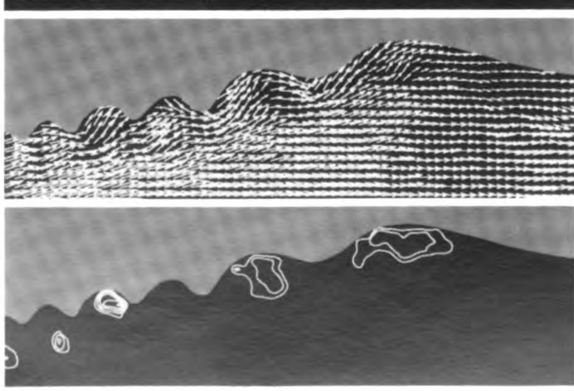

Wave instabilities and breaking. *Free-surface capillaries (images at left), at a Froude number FR = 0.43, exhibit large spatial variations of instantaneous velocity and concentrations of positive (gray) and negative (white) vorticity beneath their troughs and crests. An increase to Fr = 0.56 generates a fully-evolved breaker, represented by the instantaneous velocity in the laboratory frame (top image), and a frame moving at one-third the inflow velocity (middle image). Instantaneous vorticity concentrations are evident in the separated mixing-layer formed by the onset of breaking (bottom image). From the laboratory experiments of Lin and Rockwell (Physics of Fluids 6(9), p.2877 and JFM 302, p.29).*

Naval Research Reviews

Office of Naval Research
Two/1996
Vol XLVIII

This *Naval Research Reviews* on the topic of nonlinear ocean waves is published in two companion issues, Two/1996 (pages 1-28) and Three/1996 (pages 29-72). The introduction which puts the six articles into context and provides an historical perspective appears at the beginning of Two/1996.

Articles

About the Cover

(Top) An image from the Marseilles, France wind/wave facility of short gravity-capillary waves generated under wind conditions of 6.3 m/s and 5 m fetch. Wind forcing is left to right with yellow and red colors indicating wind slope in wind direction and green and blue indicating wave slope in the cross-wind direction. Cusp-shaped bores are seen to generatic short parasitic capillary waves in the direction of propagation that are thought according to current models to produce regions of high vorticity. Citation: Jaehne, B. And K. Riemer, "Two-dimensional wave number spectra of small scale water surface waves," J. Geophysical Research, v95, 11531-11546.
(Bottom) A model by Michalel Milder for the generation of short waves under constant wind forcing produced this similar image. The model incorporates gravity-capillary wave interations through a surface wave Hamiltonian approach. Citation: Milder, D.M., "An improved formalism for wave scattering from rough surfaces," J. Acoustical Society of America, v89, 529-541.

Naval Research Reviews publishes articles about research conducted by the laboratories and contractors of the Office of Naval Research and describes important naval experimental activities. Manuscripts submitted for publication, correspondence concerning prospective articles, and changes of address, should be directed to Code OPARI, Office of Naval Research, Arlington, VA 22217-5000. Requests for subscriptions should be directed to the Superintendent of Documents, U.S. Government Printing Office, Washington, DC 20403. *Naval Research Reviews* is published from appropriated funds by authority of the Office of Naval Research in accordance with Navy Publications and Printing Regulations. NAVSO P-35.

FOCUSED ISSUE ON NONLINEAR OCEAN WAVES

Guest Editors: Louis Goodman
Michael Shlesinger
Thomas Swean

Most of the surface of the earth is covered by water and most of the time this surface is in motion in the form of water waves. Surface waves influence the performance of all Naval Systems that operate on, through, or near the ocean interface and are central to a wide range of geophysical issues as well. Nonlinear wave behavior is important to nearly all Navy concerns regarding surface waves including remote sensing, acoustic propagation, extreme wave loads, reliability and seaworthiness, sediment transport and near-shore operations. Improvements in Naval capabilities to operate in the ocean environment depend significantly on advancing the understanding of nonlinear ocean wave generation and evolution. This is the subject of this focused issue of the *Naval Research Reviews*.

The mathematical theory of surface waves has been actively developed since the 1800's. The theory is complex. Fundamentally, this is because the instantaneous shape of the interface is both a boundary condition and a solution to a nonlinear partial differential equation. Furthermore, the time-dependent shape of the ocean surface is affected by wind conditions, underwater currents, internal waves and bottom topography. Classical approaches have generally exploited the underlying linearity of the nonlinear system, weak nonlinearities, and specialized nonlinear solutions such as solitary waveforms. It is now recognized that further advances in the fundamental issues of ocean wave dynamics necessitates investigation of problems that are often highly nonlinear, and even turbulent and chaotic. The significance and challenge presented by these nonlinear problems resulted in the development of a five-year program on nonlinear ocean waves which began in 1992. Major topics of interest have been wave generation and growth, wave-wave interaction, wave-seabed interaction and wave breaking. New theoretical approaches based on extending and applying the ideas of nonlinear dynamics and chaos have been brought to bear on these problems. Emerging data analysis techniques (e.g. wavelets, inverse scattering transforms, higher order spectral transforms) have been further developed and applied to field and laboratory data as well as to solutions of nonlinear partial differential equations governing nonlinear wave behavior.

Our issue starts off with a beautiful review by Professor Mei on the many time and length scales found in ocean wave dynamics. He summarizes some of the recent advances in understanding the interactions among different scales and stresses the practical implications this new understanding portends for coastal engineering. Dr. Huangs article tells of the importance of laboratory wave tank experiments in identifying and studying many of the controlling mechanisms of wave dynamics. He reminds us that most theoretical advances have been inspired by direct observation of wave phenomena and that cleverly designed laboratory experiments constitute the bulk of these observations.

Our next three articles review important analysis techniques that have been applied to the ocean surface wave problem. Professor Spedding reviews the application of two dimensional wavelet transforms for analyzing ocean waves. The wavelet has the advantage of providing local information, whereas the conventional power spectrum localizes in frequency but mixes all spatial information. Professors Elgar, Herbers and Guza review bispectral techniques to study correlation and energy transfer in triads of waves and discuss their application to near-shore wave dynamics to gain insight into the nonlinearities of wave interactions. Professor Osborne reviews aspects of inverse scattering theory and shows how new developments have resulted in remarkable simplifications to the use of inverse scattering transforms for the study of nonlinear water waves. He uses this technique to identify soliton behavior in shallow water waves. This information is not readily available or accessible through other approaches. Together these techniques provide the modern researcher with a new and more powerful array of tools with which to look at ocean wave data from a fresh perspective.

With the exception of studies directed specifically at the generation of waves by wind, the classical theories have generally ignored the dynamics of the air and neglect the possibility of shear in the water. However, it has become recognized that there may be a number of important phenomena where air and water shears play major roles. Our final article, contributed by Professors Caponi and Saffman, describes recent major advances in understanding the effect of wind and water shear on surface waves. The interplay of long and short waves with wind and shear generates a variety of nonlinear behaviors whose understanding is important for interpreting radar images of the ocean.

With each issue of the *Naval Research Reviews* we highlight a person who has contributed substantially and consistently to the subject at hand. In this issue we honor Professor Marshall Tulin with a brief biographical note and a sketch of his likeness.

The articles in this issue of the *Naval Research Reviews* represent but a sampling of this work; however, we hope they will provide the reader with a good overview of the state-of-the-art understanding of the complex behavior of nonlinear waves. It is certain the reader will develop an increased appreciation of ocean wave dynamics as one of the most exciting and sophisticated areas of scientific investigation, and one with immense practical importance as well.

Multiple-scale Dynamics of Ocean Surface Waves - Physics and Engineering Applications

Chiang C. Mei
Department of Civil and Environmental Engineering
Massachusetts Institute of Technology
Cambridge, MA

Introduction

One of the most distinguishing features of ocean surface waves is the existence of many contrasting length and time scales. If one scale is examined at a time, the physics can be easily studied, either by theoretical means or in the laboratory. The interactions among different scales are, however, basic to the variety and complexity of natural phenomena. In the past few decades, giant strides have been made on these interactions, especially when nonlinearity plays a role.

In this review we shall summarize some of the interesting advances, with particular emphasis on the dynamical effects of weak nonlinearity, whose influence is, however, not always weak over sufficiently long temporal or spatial scale. Selected topics relevant to both oceanographic and engineering interests will be discussed, with a view to highlighting not only the commonality of scientific ideas and techniques but also to sitimulating further interactions between ocean scientists and engineers.

We begin with the interaction between short and long waves, a topic of key importance to the development of the sea spectrum. A partial impetus for studying this topic stems from the need for proper interpretation of satellite images from radar signals backscattered from the sea surface. These radar waves are usually in the wavelength range from centimeters (X-band) to tens of centimeters (L-band), and are too short to penetrate much below the sea surface. Nevertheless, revelations of detailed bathymetric features of the sea bottom by these images suggest the possible role of long-scale modulation of short surface waves by long waves or currents, which are directly affected by bathymetry.

The physics of short and long waves is relatively easy to analyse if one or both are of small amplitude. Much insight can be gained by studying either weak long waves generated by much stronger short waves, or short waves riding on stronger long waves (with currents being a limiting case). These topics are separately discussed in the sections to follow.

Figure 1.

Wave spectra recorded at Barbers Point Harbor, Hawaii, 1989, by Hawaii District Office, Corps of Engineers. Records in the lower (higher) frequency half of the diagram were taken from a station inside (outside) the basin.

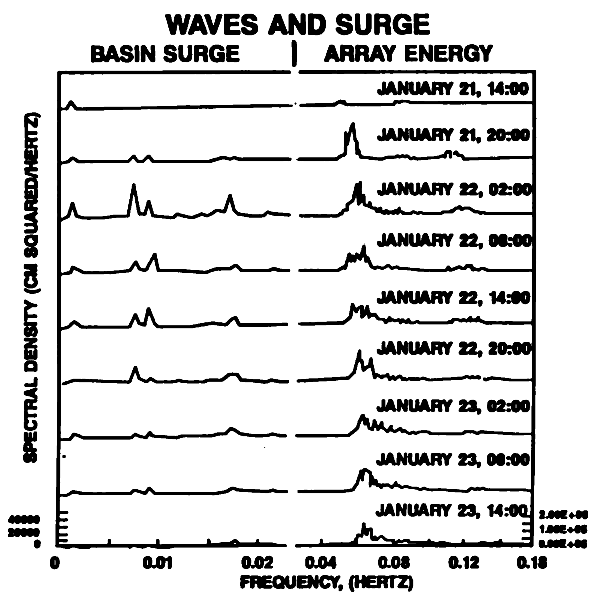

While the science of ocean waves captivates oceanographers and engineers alike, the latter are motivated more often by phenomena affecting or affected by man-made structures. Practical interests in coastal engineering require the understanding of long-period resonance of harbors when the incident wind waves have much shorter periods. Prediction of slow-drift oscillations of tension-leg platforms must be based on a sound understanding of long-period waves affected by the interaction of short-period wind waves and the floating structure. In the last three sections we discuss some nonlinear wave problems arising in wave/body interactions.

The dynamics of ocean surface waves is a broad topic. Several important aspects not covered here have fortunately been surveyed in scattered articles. For example the dynamics of the breaking waves in the surf zone has been reviewed by Battjes(1988). Many topics of coastal wave dynamics including the formation of sand ripples are surveyed in Mei and Liu(1993). Recent developments on wave transformation from deep to shallow water can be found in Liu(1994). For deeper and more general expositions one may consult Phillips (1978) for oceanographic applications, Mei(1989) for coastal and ocean engineering, and Debnath (1994) for recent mathematical advances.

Short and Long Waves

Long waves generated by short waves

For moored ships, tethered offshore submercibles, or tension-leg platforms, it is important to know when to expect resonant excitation by incident seas. Since the natural periods of many mooring systems often fall in the range of 1 to 10 min., sea waves of similar periods, called *infragravity waves* for their much greater length compared to the usual wind waves, are therefore of considerable interest to engineers. How are these infragravity waves originated? How do they propagate over complex bathymetry or coastlines? Do they affect the evolution of bathymetry or coastlines?

One source of infragravity waves is nonlinearity. In particular, through second-order interactions any two waves of different frequencies from the energetic part of the wind-wave spectrum can force waves at the sum frequency $\omega_1 + \omega_2$ and at the difference frequency $\omega_1 - \omega_2$. If the spectrum is narrow-banded, the difference frequency corresponds to a very long period, which would induce long waves in finite depth. In their classic theory on radiation stresses, Longuet-Higgins and Stewart (1960) have shown that a slowly modulated group of short waves must be accompanied by a mean-sea-level setdown, whose (negative) amplitude is proportional to the square of the local wave amplitude and moves at the group velocity of the short waves. The set-down is therefore a long wave bound to the envelope of the short waves.

The radiation stresses are essentially the averaged rate of momentum fluxes due to wave fluctuations when the averages are taken in depth and over the period of the short waves. The basic idea is similar to Reynolds equations by averaging over random fluctuations of turbulence. In particular, when the short waves are gentle, the equation governing the long-wave surface displacement is of the form:

$$\frac{\partial^2 \zeta}{\partial t^2} - g\frac{\partial}{\partial x_j}\left(h\frac{\partial \zeta}{\partial x_j}\right) = \frac{1}{\rho}\frac{\partial^2 S_{ij}}{\partial x_i \partial x_j},$$

where S_{ij} are the radiation stress components, being the correlations of velocity components. In turbulent flows the Reynolds stresses are not known a priori, and additional hypotheses are needed to enable the computation of mean-flow quantities. Whenever breaking is absent and wave amplitudes are small, the radiation stresses can be calculated by using the linearized theory of waves. Thus, the long-wave displacement must be of second order in wave steepness and can be solved as a linear problem with known forcing.

Among the earliest applications of this theory we may include surf beats in one dimension (Longuet-Higgins and Stewart, 1960) and the long-shore current in the surf zone, where empirical assumptions are added for the breaking waves (Bowen, 1969; Longuet-Higgins, 1970a,b). The mean-flow

Figure 2.

Reflection coefficient of waves over sincusoidal bars on a horizontal bed. In the experiments by Heathershaw (1982) sinusoidal bars of fixed amplitude b and 1 m wavelength cover the region from x = 0 to 10 m. Incident wavelength is 2 m. Four different water depths h were tested. The theory of Mei (1985) is shown in solid lines.

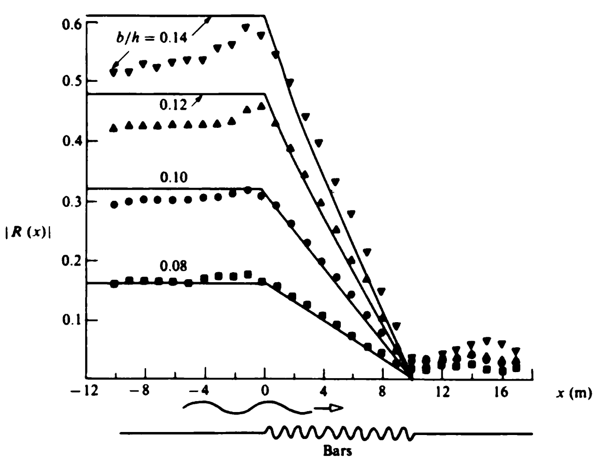

problems are reducible to steady states. Molin (1982), Mei and Benmoussa (1984), and Liu (1989) have applied the theory to narrow-banded waves refracted by slowly varying submarine ridges and canyons. They found that in a shoaling water the incident wave group and the long setdown wave, which are aligned in constant depth, propagate in different directions upon entering the zone of variable depth. Furthermore, there is another long wave propagating at the speed of $\sqrt{gh}$ of the linearized long waves. The second long wave corresponds to the homogeneous solution of (2.1) and may be termed the free long wave, to be distinguished from the group-bound long waves. Free long waves can propagate into regions where there are no short waves, whose absence may be the consequence of reflection or diffraction by bathymetry or lateral boundaries. A number of interesting scenarios may occur when groups of short waves propagate from a zone of constant depth to a zone of variable depth. For example, if the short waves of a certain carrier frequency advance obliquely toward a deep canyon, they can be first refracted and then reflected at a caustic so that they do not cross the canyon. However, free long waves can enter and pass the canyon. In the case of a submarine ridge, the short waves pass the ridge but free long waves can be trapped on the ridge (Mei and Benmoussa, 1984; Agnon and Mei, 1988). Short waves incident on a large island should not be significant deep inside the shadow, but the long waves can creep in there (Zhou and Liu, 1987). If groups of short waves enter a harbor, free long waves can be created at the harbor entrance and be resonated inside. This phenomenon has been experienced in many harbors where tsunamis are of no concern. A record of this phenomenon is shown in Figure 1, where the wave spectra from gages outside and inside the Barbers' Point Harbor, Hawaii, are superimposed. While the records taken at a station outside give only the high-frequency peaks, the low-frequency peaks are found at a station inside the harbor. Theories for such phenomenon are still at their infancy (Mei and Agnon, 1989; Wu and Liu, 1990).

Along some beaches such as the Chesapeake Bay, there are many alongshore bars running parallel to the coast. Bragg resonance can cause strong reflections of the incident waves if the spacing between bars is roughly one-half that of the incoming sea waves. This was measured in the laboratory by Heathershaw (1982) and predicted theoretically by Mei (1985). Figure 2 shows the spatial variation of the reflection coefficient over ten sinusoidal bars. This strong reflection has at least two nonlinear effects. One is to induce a circulation in the bottom boundary layer, and one is to create long waves, both bound to the short wave envelope and free with the speed $\sqrt{gh}$. The first effect is the result of time-averaged Reynolds stresses due to friction in the bottom boundary layer. Very close to the seabed the induced drift current converges toward the points directly beneath the maxima of the wave envelope; near the top of the boundary layer, the drift current converges toward the points beneath the minima of the wave envelope. Thus, heavy sand particles rolling on the seabed are transported toward the envelope minima to form or to heighten the crests of sandbars. Since these extrema are separated at half of the incident wavelength, the wavelength of sand-bars is roughly one half of that of the waves. Light particles in suspension are transported toward the minima of the wave envelope. With more deposition at the crests, parallel bars grow in height and increase the reflection by Bragg resonance, which in turn further enhances the growth of existing bars and the birth of new bars (see Mei, 1989, p. 433). Thus the increase of wave reflection and the growth of sandbars are cause and effect of each other. As another consequence, sand particles of different diameters are segregated so that coarse sands are more abundant near the bar crests and fine sands near the troughs; this phenomenon is called sediment sorting.

The second nonlinear effect is the result of radiation stresses in the inviscid core, and is present when the incident waves are narrow-banded. Then scattering of short waves is accompanied by the scattering of bound long waves and the radiation of free long waves. If the barred region is sufficiently wide, nearly complete reflection of short waves is possible, leaving only the free long wave on the transmission side (Hara and Mei, 1987). The longshore bars can, therefore, act like a magic wall that separates a concert hall: violins played on one side sound like cellos on the other. An experimental confirmation of the theory is shown in Figure 3(from Hara and Mei, 1987). More research is definitely needed to couple the dynamics of the sediments with that of the waves.

Figure 3.

Evolution of a group of waves arriving from $x < 0$ and Bragg-reflected by periodic bars extending from $x = 0$ to 12 m on a horizontal seabed. The experimental data are shown in solid curves; the theoretical wave envelopes are shown by dashed curves. Note the dispersion of the incident wave envelope A and the reflected wave envelope B. Also shown are the second-order long wave trace ζ_{20}. From the record a x = 12 m, the long wave arrives earlier than the short wave envelope, implying the presence of the free long wave.

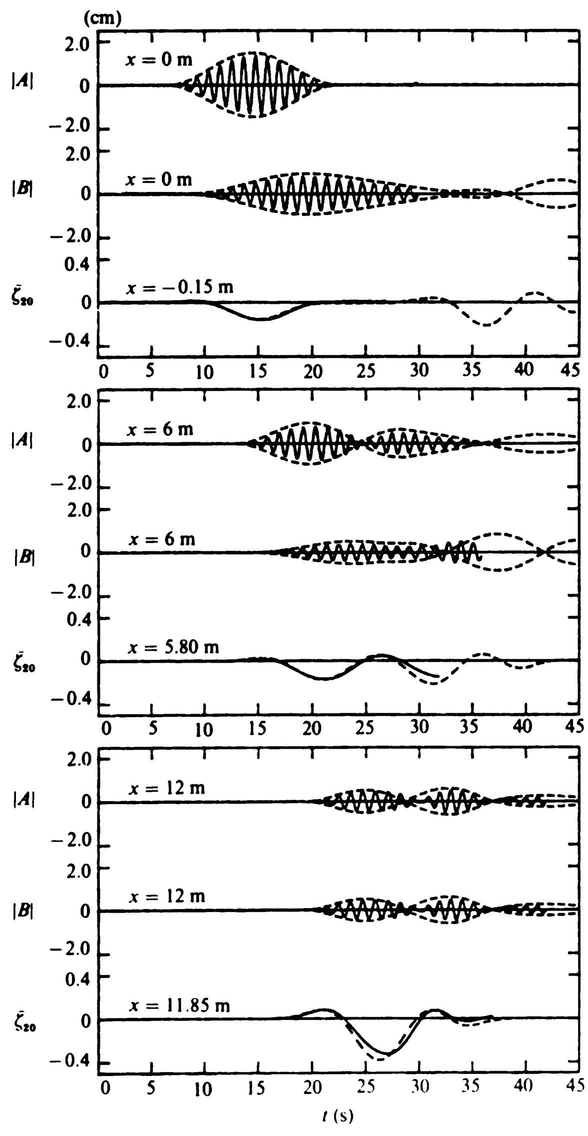

Modulation and instability of short gravity waves riding on a long wave

For weak interactions between two wavetrains of different lengths and low amplitudes, Longuet-Higgins and Stewart (1960) have shown that short waves become steeper near the long-wave crests and flatter near the long-wave troughs. In developing their theory, Taylor expansion about the horizontal mean surface is made, thus the contrast in amplitudes and wavelengths between the two wavetrains must be limited. On a finite amplitude long wave, the modulation of a train of collinear short waves of infinitesimal amplitude has been studied by Longuet-Higgins (1987), who calculated the long wave by numerical means. Henyey, et al. (1988) used a Hamiltonian formalism and deduced the action conservation principle for infinitesimal short waves. Zhang and Melville (1990) went beyond linear modulation to account for higher-order effects in short waves and obtained a nonlinear Schr "odinger (NLS) equation for the short-wave envelope. Some coefficients in the NLS equation have slowly varying coefficients representing the effects of long waves. They used the result to find the envelope of a Stokes wave, which remains steady with respect to the long wave.

As was pointed out by Longuet-Higgins (1987), an effect of the long wave is to provide an oscillating gravity field for the short wave. Standing waves in a vertically oscillating basin are known to exhibit subharmonic instability. Similar instability must therefore be expected in short gravity waves riding on a long wave. Naciri and Mei (1992) first re-examined the linear effects of a long wave on the modulation of infinitesimal short waves over a time span of a few long-wave periods, and then studied the sideband instability as well as the subsequent nonlinear evolution of Stokes waves over many long-wave periods. Since sideband instability is a special case of quartet resonance discovered by Phillips (1960), this example gives some insight on the effects of a long wave on resonant interactions.

Let k, ω and A be the wavenumber, frequency and amplitude of the short wave and K,Ω and B be the corresponding quantities of the long waves. Then for infinitely deep water, $\Omega=\sqrt{gK}$ and $\omega=\sqrt{gk}$. If the wave frequency contrast is $\Omega/\omega = O(\varepsilon) << 1$, then the wavenumber contrast must be $K/k = O(\varepsilon^2)$. Moreover, if the short waves are gentle but the long waves are steep, $kA=O(\varepsilon) << 1$ and $KB=O(1)$, then $kB = O(1/\varepsilon) >> 1$, so that the short wavelength is much less than the long-wave amplitude. A Taylor expansion cannot be made from the horizontal mean sea level but must be made from the long-wave surface. Instead of using orthogonal coordinates conforming with the long-wave surface, Lagrangian coordinates can be used, where the fluid motion is described by the instantaneous positions of all fluid particles: $X(a,b,c,t), Y(a,b,c,t) Z(a,b,c,t)$, where (a,b,c) refer to the initial position of a particle. The usual kinematic boundary condition

Figure 4.

Linear growth rate of sidebands as a function of short wave parameter α and the sideband wavenumber ν for a long wave with $KB = 0.3$. The short wave steepness is $\kappa A = 0.13$.

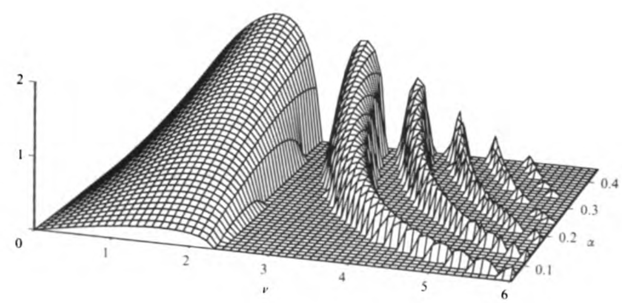

that a fluid particle on the free surface must never leave the free surface can be stated simply by designating the free surface as c=0. To avoid excessive computation, Naciri and Mei (1992) further modeled the long wave by Gerstner's simple but exact two-dimensional solution

$$x=a+B\sin(\Omega t-Ka)e^{Kc},\quad z=c+B\cos(\Omega t-Ka)e^{Kc} \qquad (2.2)$$

with $\Omega^2=gK$. It is well known that the Gerstner wave has finite vorticity that attains the maximum at the free surface c=0 and is counterclockwise if the wave propagates to the right; therefore, it cannot be the result of wind blowing in the same direction of the wave.

For a nearly sinusoidal short wave superimposing on Gerstner's long wave, the evolution equation reads, in normalized form,

$$\frac{\partial A}{\partial \varphi}=-\frac{1}{\delta}\frac{K\sin\varphi}{1-2KB\cos\varphi+K^2b^2}\left[1+\frac{\Omega}{\sigma}\frac{1+2KB\cos\varphi-3K^2b^2}{1-2KB\cos\varphi+K^2b^2}\right]$$
$$-\frac{i\alpha}{4}\frac{\partial^2 A}{\partial \xi^2}-\frac{i\alpha|A|^2A}{1-2KB\cos\varphi+K^2B^2} \qquad (2.3)$$

where

$$\alpha=\frac{1}{2\delta}\frac{\sigma}{\Omega}(k\bar{A})^2\,, \qquad (2.4)$$

with $\bar{A}$, σ, k being the characteristic amplitude, frequency and wavenumber of the short waves, and

$$\delta=1-\frac{\Omega}{2\sigma} \qquad (2.5)$$

and

$$\varphi=\Omega t-Ka\,. \qquad (2.6)$$

The normalized coordinate φ can be as large as $O(\varepsilon^{-1})$, where $\varepsilon+O(\Omega/\omega, k\bar{A})<<1$.

For $\varphi=O(1)$, i.e., with a few long-wave periods, all $O(\varepsilon)$ terms can be ignored as a first approximation

$$\frac{\partial A}{\partial \varphi}=\frac{-KB\sin\varphi}{1-2KB\cos\varphi}A\,, \qquad (2.7)$$

which can be solved to give

$$\frac{|A|}{\bar{A}}=\frac{1}{\sqrt{1-2KB\cos\varphi+K^2B^2}} \qquad (2.8)$$

Figure 5.

Typical evolution of short wave envelope riding on a long wave. (a) The Fourier domain where A_0 is the amplitude of the carrier wave, A_1 is the amplitude of the sideband, and A_2, A_3,... are the higher harmonics of the side bands. (b) The physical domain while ϕ is the time and ξ the spatial coordinate moving at the group velocity. Note the spatial-temporal chaos.

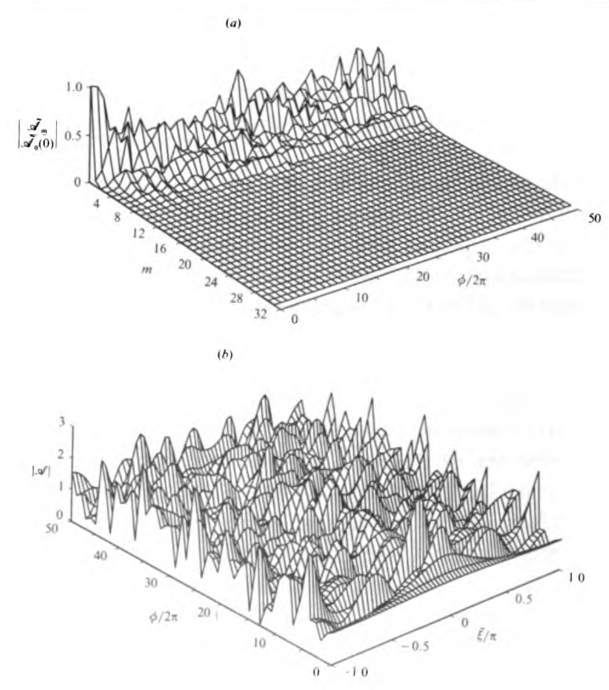

Figure 6.

Dispersion relation for capillary-gravity waves on a current. For fixed ω and U, the wavenumber κ is given by the intersection of the straightline ω - κU and the curve $\sigma(\kappa)$. In Fig. 6.a, there is only one interaction at κ_1. In Fig. 6.b, there are three intersections at κ_1, κ_2 and κ_3, with $\kappa_1 < \kappa_2 < \kappa_3$.

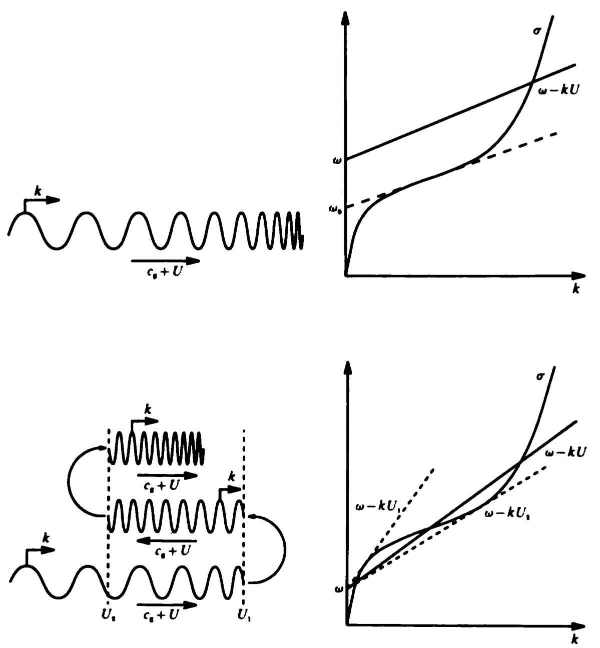

This simple formula agrees well with Longuet-Higgins' (1987) numerical solution of irrotational Stokes wave with KB up to 0.3.

The Stokes waves envelope A_s (φ) can be regarded as the solution of (2.3) independent of ξ and can be obtained explicitly. Sideband perturbances are governed by a linear partial differential system with periodic coefficients and can be studied with the aid of the Floquet theory.

As a sample result from Naciri and Mei (1992), we show in Figure 4 for $kA = 0.13$, $\Omega/\sigma = 0.07$, which corresponds to α=0.135, the effects of KB and the sideband wavenumber ν. When the long wave is absent, KB=0, the band of instability reduces to that of Benjamin and Feir (1967) with the bandwidth given by $0 \le \nu \le 2\sqrt{2}$. When KB increases, new bands of instability appear and the maximum growth rate increases. When the sidebands of the fundamental harmonic are unstable, their higher harmonics may also easily fall into one of these new bands of instability. Great complexity in the nonlinear stage can, therefore, be expected. A sample numerical result in Figure 5 (from Naciri and Mei, 1992) shows spatio-temporal chaos. As α increases, the trend toward chaos amplifies. Thus, by the inherent nonlinearity on the ocean surface, long-wave modulation of narrow-banded short waves can contribute to randomness with scales much greater than the characteristic wavelength. This mechanism is, therefore, complementary to the randomization of smaller scales due to wind input and/or turbulent mixing.

Instability of collinear short waves on a long wave due to oblique sidebands has also been studied by Naciri and Mei (1994), but nonlinear evolution has not been examined. A quick turn to spatio-temporal chaos is expected, which renders the assumption of slow modulation inaccurate. Other theoretical approaches allowing broad bands are needed.

Reflection of capillary-gravity waves by a nonuniform current

When short capillary-gravity waves are reflected by a long wave or a nonuniform current, striking physics may arise. In a flume with a sloping bottom, Pokazeyeu and Rosenberg (1983) and Badulin, Pokazeyeu and Rosenberg (1983) first produced a steady and nonuniform current with speeds in the range of 4-24 cm/s flowing from shallow to deep water. In the direction of intensifying current (from deep to shallow water), wave packets of 2-11 Hz carrier frequency were sent. Along with complete blockage by the opposing current, the waves are found to be shortened by orders of magnitude. Because shorter waves are more easily damped by viscosity, the much shortened waves can be completely annihilated without the help of breaking (Phillips, 1981). Badulin, et al. (1983) further observed the phenomenon of double reflection with drastic shortening after each reflection.

As explained by Badulin, et al. (1983), the shortening can be understood by examining the dispersion relation. For an opposing current with local speed $U < 0$, the dispersion relation is

$$\omega + k\,|U| = \left(gk + \frac{Tk^3}{\rho}\right)^{1/2} \equiv \sigma(k)\,. \qquad 2.9$$

In Figure 6, the function $\sigma(k)$ is represented by the curve, while the left-hand side by the straight line with the slope $\omega/k = |U|$. Their intersection gives the wavenumber of the short wave. Let ω_o be the intersection of the straight line tangent to the σ curve at the point of inflection. We can distinguish two cases.

(i) $\omega > \omega_o$: As shown in Figure 6.a there is only one intersection at the wavenumber $k_1 > 0$ which increases with $|U|$. Hence, there is only one wave propagating into the current. As it propagates forward to the shallow water, waves becomes shorter. Since $d\sigma/dk > -U$, $C_g + U > 0$, - U, C_g+U 0, energy is propagated forward into shallow water also.

(ii) $\omega < \omega_o$: In the region where $|U| < |U_2|$, there is only one solution k_1. Again, $d\sigma/dk + U = C_g + U > 0$, signifying forward propagation of wave phase and energy in the current.

As the wave enters the zone of stronger current $|U_2| < |U| < |U_1|$, three waves coexist: $0 < k_1 < k_2 < k_3$ (Figure 6.b). For k_1 and k_3 $d\sigma/dk > -U$, so that the energy is transported forward. For k_2, however, $d\sigma/dk > -U$, hence energy is reflected. As $|U|$ further increases beyond $|U_1|$, i.e., $|U| > |U_1|$, only the shorter wave (k_1) can exist with energy transported forward.

In summary, there are two points of reflection: one at x_2 (where $U=U_2$) and one at x_1 (where $U=U_1$). Between them k_1 can be regarded as the incident wave, k_2 the reflected wave, and k_3 the transmitted wave. The wavelength is greatly reduced after each reflection.

This problem can be analyzed by the uniformly valid theory of Shyu and Phillips (1992). Trulsen and Mei (1993) employed a WKB approximation away from, and boundary-layer corrections near, the reflection points. With a crude account for viscous damping, the dramatic shortening and effective annihilation of a long-wave packet after double reflection can be clearly seen in Figure 7 (from Trulsen and Mei, 1993).

Triad resonance of capillary-gravity waves affected by a long wave

At the beginning of this century Harrison (1909) and Wilton (1915) found that a monochromatic progressive capillary-gravity wave can excite its second harmonic to significant amplitude. Half a century later McGoldrick (1965) found this phenomenon to be a special case of nonlinear triad resonance, where three capillary-gravity wavetrains can resonantly exchange energy among one another through quadratic coupling. After the seminal works by Phillips (1960) on gravity waves and by McGoldrick (1965) for capillary-gravity waves, the study of nonlinear resonance has mushroomed. For a comprehensive survey, see Craik (1985).

The effect of long waves on a resonant triad of capillary-gravity waves has been treated recently by Trulsen and Mei (1995), who also used Lagrangian coordinates and made the following order assumptions: $kA = O(\varepsilon)$ $KB = O(\varepsilon)$ $K/k = O(\varepsilon^2)\Omega/\omega = O(\varepsilon)$. With these scale choices, both short and long waves are gentle in slope. By ignoring viscous damping and applying the multiple-scale analysis to the second order, three evolution equations are derived:

$$\frac{\partial A_1}{\partial t} + C_{g1} \cdot \nabla A_1 + i\beta_1 A_1 \cos\varphi + i\alpha_1 A_2^{*} A_3 + 0 \qquad (2.10)$$

$$\frac{\partial A_2}{\partial t} + C_{g1} \cdot \nabla A_2 + i\beta_2 A_2 \cos\varphi + i\alpha_2 A_1^{*} A_3 + 0 \qquad (2.11)$$

$$\frac{\partial A_3}{\partial t} + C_{g3} \cdot \nabla A_3 + i\beta_3 A_3 \cos\varphi + i\alpha_3 A_1^{*} A_2 + 0 \qquad (2.12)$$

The terms representing interactions between short and long waves are $\beta_i A_i \cos\varphi$, where β_i is proportional to the long-wave amplitude and $\varphi = -\Omega t$ is the long-wave phase. Trulsen and Mei (1995) focused their attention to the case with spatial uniformity so that an ordinary dynamical system of the sixth order is obtained. By a judicious transformation and the use of conser-

Figure 7.

Snapshots of waves advancing into an opposing current. From the top figure to the bottom, time increases. Damping is included. Note the annihilation of waves after second reflection.

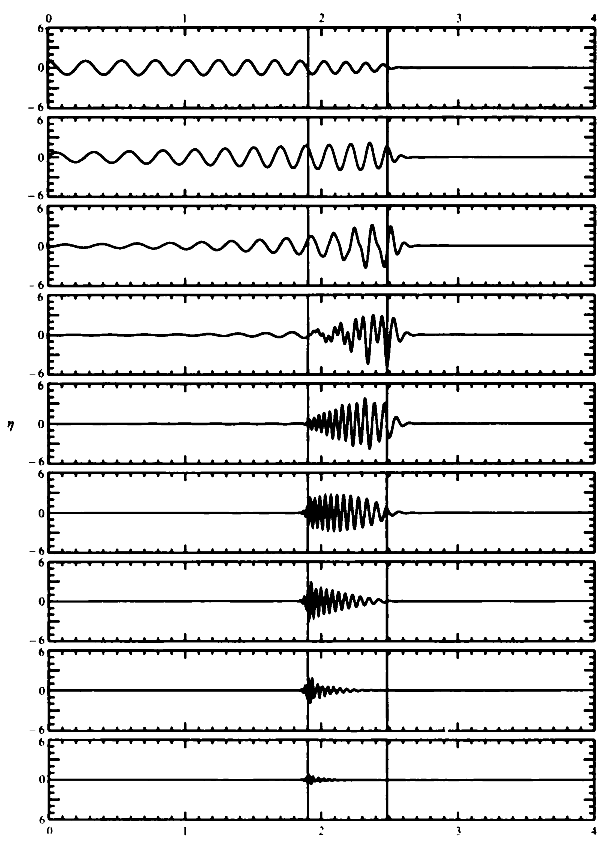

vation laws, the number of independent variables is reduced to two, yielding

$$\frac{dj}{dt} = -r\,[(1-j)\,j\,(j+j_*)]^{1/2}\sin\varphi \qquad (2.13)$$

and

$$\frac{d\psi}{dt} = r\cos\psi\,\frac{3j^2-2j+2j_*j-j_*}{2[(1-j)\,j\,(j+j_*)]^{1/2}} + \Delta + \beta\cos t \qquad (2.14)$$

where j is proportional to the wave action of the shortest wave in the triad, and $\psi=\varphi_1+\varphi_2-\varphi_3$ is a special combination of phase angles of the wave actions. Because of the omission of viscosity, the system is Hamiltonian. Without long waves the above Hamiltonian system is autonomous and may be solved exactly. For weak long waves, a perturbation analysis is possible, which shows various possibilities of bifurcations and modulational resonances of superharmonic or subharmonic varieties at certain long-wave frequency. As the long-wave amplitude increases, these resonances lead to homoclinic orbits, horseshoe tangles, and chaos, as is expected of a Hamiltonian system. A sample result is shown in Figure 8 (from Trulsen and Mei, 1995). This study shows again that a long wave triggers chaos among nonlinearly resonating waves. Further studies of equations (2.10-12) on the spatio-temporal chaos are worthwhile.

Frequency downshift and long-time modulation

The prediction of the spectral development of wind-induced waves is the primary goal of wave-modeling, which is immensely important to engineering and oceanography. In this task one must integrate the mechanisms of wind input, wave/wave interactions and dissipation due to breaking, internal and bottom friction, etc. Based on existing theoretical, laboratory and field knowledge of these mechanisms, impressive progress has been made, resulting in the third-generation model for wave prediction (Koman, et al., 1995). On the other hand, a deeper understanding is also being pursued by studying separately various aspects of the whole phenomenon.

One prominent feature of a wind-wave spectrum evolution is called the *frequency downshift*. Under stationary offshore wind, the frequency at the peak of the energy spectrum of wind-generated waves is known to steadily decrease with increasing fetch, while the peak height increases. From JONSWAP measurements, the peak frequency varies with fetch according to

$$f_m = 3.5\,(gx/U_{10})^{-0.33} \qquad (3.1)$$

where x denotes the fetch, and U_{10} denotes the mean wind speed 10 m above the mean sea level. The cause of the downshift of peak frequency has been the focus of attention by various authors in recent years.

In their experimental study of the Benjamin-Feir instability of uniform Stokes waves, Lake, et al. (1977) sent steep waves down a flume of 40-foot length. For Stokes waves of relatively low initial steepness, unstable sidebands grew at equal rates. The time scale of growth decreases with the square of wave steepness. However, for steeper waves the most unstable sidebands grew at equal rates only near the wavemaker. Further downstream the lower sideband becomes higher than both the upper sideband and the carrier wave. As a consequence, the spectral peak shifts to a lower frequency. Without breaking, there is a tendency for the carrier to regain its strength and for the sidebands to diminish further down the tank. Melville (1982) performed similar experiments in a longer flume with steeper waves. He observed not only faster growth of the lower sideband but wave breaking at the height of modulation.

For low enough steepness, the first nonlinear stage of sideband evolution is well described by the nonlinear Schr "odinger equation (NLS)

$$i\frac{\partial A}{\partial t} + \alpha\frac{\partial^2 A}{\partial x^2} + \beta A\,|A|^2 = 0 \qquad (3.2)$$

Because of the even derivatives with respect to x, the nonlinear Schrödinger equation predicts that the sidebands, if initially equal, will grow and decay at equal rates. Using a numerical spectral method to solve the integral equation of Zakharov, which has a better accuracy than NLS, Yuen and Lake (1980) showed that the lower sideband grows faster than the upper sideband, during the initial phase of evolution. After the moment of maximum modulation, the evolution depends on the initial wave steepness. For initially gentle waves, energy in the sidebands is returned to the carrier wave, and the process of modulation and demodulation remains cyclic. For steep waves, the evolution can become chaotic. These numerical results appear to have been computed for wave-steepness too large to be consistent with the theory, however.

The instability of infinitesimal sidebands has also been studied for a steep wave by Longuet-Higgins (1987). By adding fourth-order terms to the nonlinear Schr "odinger equation, Dysthe (1979) has brought the predicted rate for an unstable growth rate closer to the more exact numerical results of Longuet-Higgins. The extension of NLS equations reads:

$$\frac{\partial A}{\partial t} + \frac{\omega}{2k}\frac{\partial A}{\partial x} + i\,\frac{\omega}{8k^2}\frac{\partial^2 A}{\partial x^2} + \frac{i}{2}\,wk^2\,|A|^2 A \qquad (3.3)$$

Figure 8.

Typical Poincare maps of the resonant triad under the influence of long wave. (a) $\beta = 0.1$, (b) $\beta = 0.2$

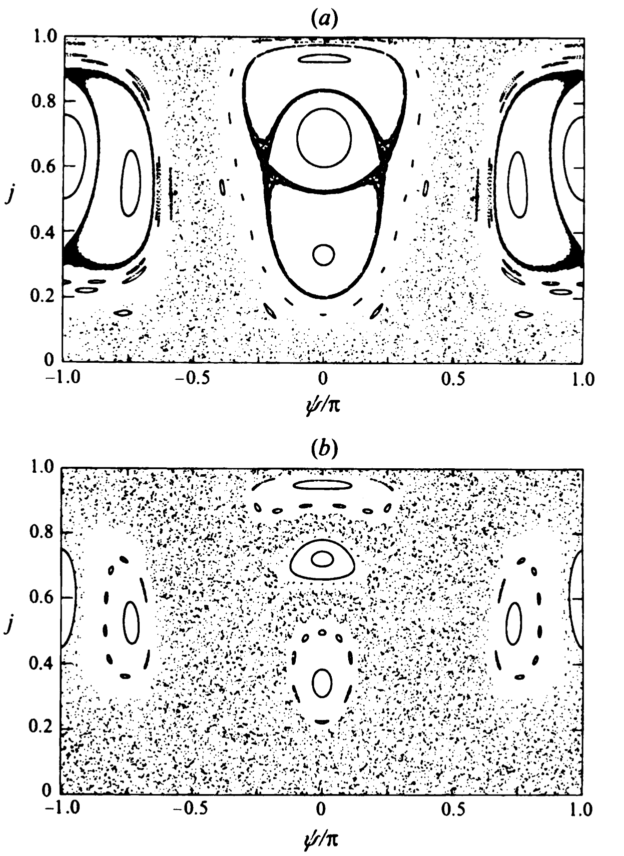

$$-\frac{1}{16}\frac{\omega}{k^3}\frac{\partial^3 A}{\partial x^3} - \frac{\omega k}{4}A^2\frac{\partial A^*}{\partial x} + \frac{3}{2}\omega k\,|A|^2\frac{\partial A}{\partial x} + ikA\frac{\partial \varphi}{\partial x}\Big|_{z=0} = 0$$

$$\frac{\partial^2\varphi}{\partial x^2} + \frac{\partial^2\varphi}{\partial z} = 0 \quad z < 0 \tag{3.4}$$

$$\frac{\partial\varphi}{\partial z} = \frac{\omega}{2}\frac{\partial |A|^2}{\partial x} \quad z = 0\,, \tag{3.5}$$

where φ represents the potential for a wave-induced current. Because of the presence of odd derivatives at the fourth order, the growth of unstable sidebands should no longer be symmetric after a long enough time of the order $k^2 a^2\omega t = O(1)$. By a numerical method Lo and Mei (1985) solved (3.3) to (3.5) for a Stokes wave with a small periodic modulation corresponding to the most unstable sidebands. They found that the initial stage of instability is followed by the faster growth of the lower sideband, which may overwhelm the carrier waves at the height of modulation. After some time energy returns from the sidebands to the carrier wave. This modulation-demodulation process goes on periodically over the time scale of $\omega t(ka)^2 = O(1)$. Lo and Mei (1985) also introduced viscous dissipation damping in the boundary layers along flume walls. The recurring trend is qualitatively unchanged. Applications of these equations are more successful in the prediction of the disintegration of an isolated wave packet into a string of smaller packets as seen in the experiments by Feir (1967).

In the flume experiments by Melville (1982), breaking is the most pronounced at the time when the sidebands attain their maximum. To simulate this effect, Trulsen and Dysthe (1990) introduced a simple model simulating energy loss by breaking, as well as wind input (1992). These two effects are represented by a pair of source and sink terms in (3.3) to (3.5). The source term is proportional to the product of wind stress and the wave amplitude. The sink term is of the relaxation type, which ensures energy loss when the wave amplitude exceeds a certain ceiling. At zero wind speed, breaking is found to preserve the dominance of the lower sideband. At higher wind speed, the higher harmonics of the lower sideband may maintain further downshift. For a still stronger wind, the carrier waves attain a critical level beyond which sidebands do not grow at all; they are overdamped. While qualitatively encouraging, the model depends on coefficients that can only be determined by curve-fitting with measurements yet unavailable. Recently, Okamura (1995) studied the evolution of standing waves and introduced two models for breaking. He notes from the experimental records of Melville and Rapp (1988) that at breaking the decreases in local velocity are much more pronounced than those in the local free-surface height. In his two models, the kinetic energy is removed when the sidebands are at their peak. The rate of removal is represented by reduction factors that are not deducible by theoretical arguments.

In a more deductive theory, Hara and Mei (1991) analyzed the downshift problem by considering weak wind and internal dissipation, but no breaking. The basic wind profile is linear but the wave-induced disturbances in air are treated as pseudo-laminar (constant eddy viscosity). By analyzing the wave-induced boundary layers in both air and water, they found that the Doppler shift caused by the wind-induced drift near the water surface must be important. The predicted effects of wind on sideband instability is reasonably well supported by the flume experiments of Bliven, et al. (1986). Furthermore, a monotonic trend of frequency downshift is found in the nonlinear stage (Figure 9, from Hara and Mei, 1991). Thus the combined effect of wind and internal dissipation can be a possible mechanism to maintain the frequency downshift.

In a subsequent paper Hara and Mei (1994) studied the linear and nonlinear phases of sideband instability of capillary-gravity waves under wind and dissipation. They found that for waves longer than $2\pi/k_*$ there is a frequency downshift after a long time. But for waves shorter than $2\pi/k_*$ there is an upshift instead. The critical number corresponds k_* to the capillary-gravity wave with the lowest phase speed and to the resonance of Wilton's ripples.

For sufficiently strong winds, internal friction is too weak to counterbalance the trend for growth; waves must break. A consistent theory must account for strong nonlinearity and turbulence in breaking waves; this task will remain a challenge to the wave scientist for some time.

We now turn to some recent studies that have strong engineering implications.

Nonlinear wave problems of engineering interest

Envelope soliton in a ship wake

Very long and narrow ship wakes of *V* shape have been revealed as bright lines in satellite photographs (Fu and Holt, 1982; Shemdin, 1990). The half angle of these wakes are typically 2^o-3^o, hence much narrower than the classical Kelvin wake with a half angle of 19.7^o. The length of such wakes can be 15-20 km. Since the relation between ships and their wakes is of obvious interest to aerial surveillance, numerous explanations have been proposed for these *V* wakes. For example, a point disturbance moving steadily in a two-layered ocean is known to generate interfacial Kelvin waves with an apex angle smaller than 19.7^o. It therefore has been suggested that these Kelvin waves can modulate the short gravity-capillary waves on the sea surface and give rise to the observed *V*-wake pattern (Tulin and Miloh, 1990). However, the modulated surface wave may be too weak to cause such a visible radar backscatter for a mild wind and a mixed-layer depth typical in the ocean (Shemdin, 1990). Another possibility is the incoherent oscillations associated with turbulence in the wake (Munk, et al., 1987). Yet another explanation attributes the *V* wake to the surface manifestation of vortices or bubbles generated from the ship's propellers. A recent theory by Gu and Phillips (1995) reasoned that the coherent structure in the turbulent jet generated by the propellers may produce oscillations along the jet boundaries, which act like oscillating pistons along the vertical center plane of the wake. These oscillations radiate two groups of small-scale surface waves that are seen as the two arms of the V wake.

The dominant mechanism of the *V* wake may be different in different observations; a single explanation may not fit all observations. To provide more definitive data, Brown, et al. (1989) conducted field tests near the coast of Southern California. Along the path of a 25-m coastguard cutter cruising at the speed of 7.7 m/s, detailed records were taken at stationary wave masts. Instead of the very narrow *V* wake, their records showed strong evidence of envelope solitons consisting of waves of frequency centered around 3.28 rad/sec. These envelopes formed *V*-like arms with a half angle 11 degrees from the ship's path, and extended roughly 1 km behind the ship. It is unclear whether these soliton wakes correspond to the much narrower and longer *V* wakes that motivated the field test; they nevertheless warrant explanation in their own right.

Much earlier, Lighthill (1967) predicted by a linear theory that a point pressure traveling on the free surface and oscillating at a constant frequency generates a Kelvin wake with a smaller apex angle than a steady Kelvin wake. Suggested by the comments of Brown, et al. (1989) that wind in the speed range of 0-6 m/sec and wind-induced swell of 0-3 m height might have been present during their field tests, Mei and Naciri

Figure 9.

Evolution of carrier wave amplitude and the sidebands under the influence of wind and dissipation. In Fig. 9.a, B_0 is the carrier wave. B_{-1} the lower sideband, and B_{+1} the upper sideband. In Fig. 9.b, $B_{\pm 2}$ are the second harmonics of $B_{\pm 1}$. Fig. 9.c gives the spectrum of wave envelope at dimensionless time τ = 50.

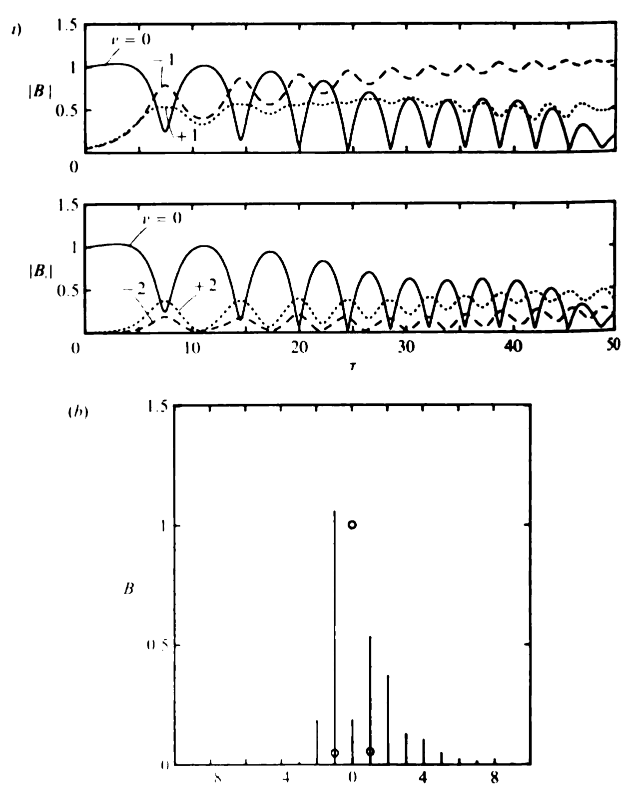

(1991) constructed a theory for a slender ship that oscillates while cruising. The ship acts as an oscillating piston advancing at a constant speed, and radiates short plane waves away from the ship. The linear part of the mechanism is therefore partially similar to that proposed by Gu and Phillips (1995). Viewed from a coordinate system fixed on the ship, the incoming head sea propagates in a current of speed V. By Doppler's effect, the ship oscillates at the encounter frequency given by

$$\omega = \omega_o \left(1 - \frac{V\omega_o}{g\cos\alpha}\right), \qquad (4.1)$$

where ω_o is the frequency of the ambient waves in a fixed coordinate system. For a head sea $\alpha=\pi$,

$$\omega = \omega_0 \left(1 + \frac{V\omega_o}{g}\right) > \omega_o , \qquad (4.2)$$

The records of Brown, et al. (1989) suggest that a head sea of ω_o = 1.5 rad/sec would give rise to a head sea of ω = 3.28 rad/sec. The ship can be induced to oscillate at the encounter frequency.

Oblique soliton envelopes are known to be solutions of the two-dimensional nonlinear Schrodinger equation. Rewritten in a moving coordinate fixed on the ship, the envelope equation is

$$\frac{\partial A}{\partial t} + C_g \frac{\partial A}{\partial x} + v\frac{\partial A}{\partial y} + i\left[\frac{\omega}{8k^2}\left(\frac{\partial^2 A}{\partial x^2} - 2\frac{\partial^2 A}{\partial y^2}\right)\right] + \frac{\omega k^2}{2}|A|^2 A = 0 , \qquad (4.3)$$

where the ship's path coincides with the y-axis and current speed V is in the positive y direction. Let $\varepsilon = kA_o << 1$. We assume the ship to be slender so that $kB=O(1)$ and $kL = O(1/\varepsilon) >> 1$ where B and L are the beam and length of the ship. Very close to the ship $kx \le O(1/\varepsilon)$ $ky = O(1)$, waves generated by the oscillating and advancing ship are described by the linear theory. In the intermediate domain $kx, ky = O(1/\varepsilon)$, the evanescent modes have lost their significance; only propagating waves remain. These outgoing waves are nearly plane waves with a finite crest length which is much greater than the wavelength, hence are slowly modulated in y and obey the linear envelope equation given by the first three terms in (4.3). In the far field where $kx = O(1/\varepsilon^2)$, $ky = O(1/\varepsilon)$, nonlinear effects become important and we must use (4.3) with the boundary condition that $A(0,y)$ is given along x=0. Transformed to a moving coordinate, the nonlinear Schr "odinger equation can be reduced and normalized to

$$-i\frac{\partial a}{\partial \eta} + \frac{1}{4}\left[1 - 2\left(\frac{Cg}{V}\right)^2\right]\frac{\partial^2 a}{\partial \xi^2} + |a|^2 a = 0 , \qquad (4.4)$$

where $a = kA$, $\xi = K A_o (kx - (Cg/V) ky)$, and $\eta = k A_o (Cg/V) ky$. By a known property of the nonlinear Schrödinger equation, solitons exist only if the coefficients in the square brackets above are positive,

$$\frac{Cg}{V} < \frac{1}{\sqrt{2}} \qquad (4.5)$$

The apex angle of the classical Kelvin wave is defined by C g/V < $1/\sqrt{8}$. Thus, if

$$\frac{1}{\sqrt{8}} < \frac{Cg}{V} < \frac{1}{\sqrt{2}} \qquad (4.6)$$

solitons exist and lie outside Kelvin's wake. Otherwise, if

$$\frac{Cg}{V} < \frac{1}{\sqrt{8}}, \qquad (4.7)$$

solitons lie inside Kelvin's wake. Since for deep water waves

$$Cg + \frac{1}{2}\sqrt{\frac{g}{k}} , \qquad (4.8)$$

a small C_g/V or a high-frequency oscillation gives rise to a small wake angle.

Mei and Naciri (1991) simulated the effect of heaving and pitching by adopting appropriate profiles for A as an initial condition for (4.4), which is then solved numerically. After a transfomration of coordinates from ξ to σ where

$$\sigma = \frac{\xi - \frac{1}{2}\xi_o}{\sqrt{1 - 2C_g^2/V_2}} \qquad (4.9)$$

with ξ_0 being proportional to the ship length L and the wave steepness $K\bar{A}$,

$$\xi_o = \frac{C_g}{V} k^2 \bar{A} L \qquad (4.10)$$

Equation (4.4) becomes

$$-i\frac{\partial a}{\partial \eta} + \frac{1}{2}\frac{\partial^2 a}{\partial \sigma^2} + |a|^2 a = 0 \qquad (4.11)$$

For a heaving ship the inital envelope close to the ship is modeled qualitatively by

$$a(\sigma, o) = sech(\sigma/\sigma_0) \qquad (4.12)$$

This profile represents a solition if $\sigma_0 = 1/\sqrt{2}$. If the ship is longer or if the oscillation amplitude is higher,the value of σ_0 is greater. In Figure 10 the spatial evolution of the initial

Figure 10.

Evaluation of soliton envelope in the wake of a heaving ship for various values of σ_0; σ_0 = 1.6 (Fig. 10a), 3 (Fig. 10.b), and 5 (Fig. 10.c).

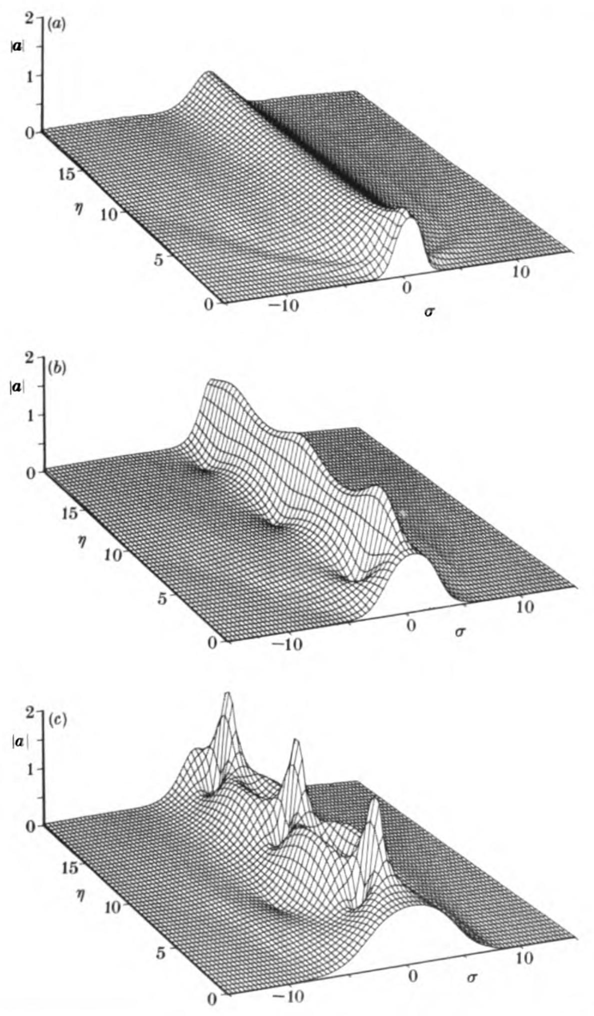

envelope on one side of the ship path is shown for several σ_0. More solitons appear for larger σ_0. The number of solitons is reflected in the number of undulations in the envelope. Whether these undulations correspond to the observations is not easy to decide on the basis of the available data. It would be interesting to check these predictions in controlled experiments in a large basin.

Upstream radiation of solitons in a channel

Nonlinear shallow water waves have been the subject of intensive scientific study in the past three decades. The seminal survey by Ursell (1953) on the long-wave paradox resolved the differences between the theories of Airy and of Rayleigh and Korteweg-de Vries. In the former, any one-dimensional compressional wave must break because the governing equations are hyperbolic. In the latter, smooth waves of permanent form can exist. The subsequent flood of activities owes much to the numerical experiments of Zabusky and Kruskal (1965) and to the use of the inverse-scattering theory to solve an initial-value problem for the Korteweg-de Vries (KdV) equation exactly. These developments have been extensively reviewed in numerous articles and books, e.g., Ablowitz and Segur (1981).

A two-dimensional extension of the KdV equation is the K-P (Kadamtsev-Petviashvilli) equation

$$(u_t + 6uu_x + u_{xxx})_x - 3u_{yy} = 0\,, \qquad (4.13)$$

which holds that if the characteristic lengths in x and y directions are related by $O(L_y) = O(L_x^2)$, numerical and analytical solutions of (4.9) have revealed the mechanics of Mach stems (Miles, 1977; Chen and Liu, 1988) and the existence of two-dimensional periodic waves (Hammack, et al., 1989).

An unusual behavior of ships in restricted water was noted in model tests before WWII by Thews and Landweber (1935) in the U.S. and Izubuchi and Nagasawa (1937) in Japan.* When a model ship is towed near the critical speed, not only does the ship residence suddenly become very large but the flow around the ship is unsteady. Here is a vivid description by Kinoshita (1946):

"When the ship speed is higher than V_g^c the whole quantity of water flowing against it can no longer pass, but .... is dammed up in front of the ship and consequently turned into backwater moving ahead of it."

Later, Graff, et al. (1964) had a similar experience in their experiments, and reported the measured ship resistance only after averaging over the time-dependent records.

Before the age of nonlinear instabilities and resonances, steady inputs were thought to produce only steady responses. Thus several authors extended the steady transonic aerodynamic theory to ship waves (Maruo, 1948; Lea and Feldman, 1972; Maruo and Tachibana, 1981). It was finally realized experimentally by Huang, et al. (1982) and numerically by Wu and Wu (1982) that the waves generated by a ship advancing

* Research in Japan before WWII was prompted by ship operations in the rivers of Chinese Manchuria under Japanese occupation. (Private communication by Professor H. Maruo of the Yokohama National University, 1985).

near the critical speed are inherently unsteady. Unlike gas dynamics, water waves are distinguished by their dispersiveness. Thus by accounting for unsteadiness, dispersion and nonlinearity, theories for two-dimensional disturbances were advanced by Wu and Wu, 1982; Akylas, 1984; Ertekin, et al., 1986; and Wu, 1987. The phenomenon is governed by an inhomogeneous KdV equation.

Replacing the near field of a ship hull by an equivalent wall-sided strut of width B, Mei and Choi (1987) showed the equation for the far field of a slender ship to be

$$\varphi_{\mu\mu} = -\left(\frac{\mu^{2-2m}}{\eta_0^2}\right)\left[2\alpha\varphi_x - 2\varphi_t - \frac{3\varepsilon}{2\mu^2}\varphi_x^2 + \frac{1}{3}\varphi_{xxx}\right]_x, \quad (4.14)$$

where all quantities are dimensionless with x normalized by the ship length L and y by the channel width W so that $\eta = y/W$. The dimensionless ratios are, respectively,

$$\varepsilon = A/h, \quad \mu = h/L, \quad \eta_o = \frac{L}{W\mu^m}$$

and α is the dimensionaless measure of detuning from the critical speed. The boundary conditions are

$$\varphi_\eta = \frac{B}{L}\frac{1}{\varepsilon\mu^m\eta_0}Y_x \text{ on } \eta = 0 \quad (4.15)$$

along the hull and

$$\varphi_\eta = 0 \text{ on } \eta = 1 \quad (4.16)$$

along the channel bank. The channel width is assumed to be $W/L = O(\mu^{-m})$ so that $\eta_0 = O(1)$. Thus, for a wide channel so that $m=1$, (4.10) is just the K-P equation, which can be solved numerically. For a narrow channel with $m = 1/2$, say, $\varphi_{\eta\eta}$ vanishes to the leading order, thus the wave field is approximately one-dimensional fore and aft. Eqn. (4.10) can be integrated to give an inhomogeneous KdV equation

$$\xi_\tau - \alpha\xi_x - \frac{3}{2}\xi\xi_x - \frac{1}{6}\xi_{xxx} = \frac{1}{2}\beta Y_x, \quad (4.17)$$

where $\xi = -\varphi_x$.

Mei (1986) used (4.13) to predict the one-dimensional upstream solitons measured by Ertekin and found good agreement despite the blunt bow of the model ship and the two-dimensional waves in the wake. By using matched asymptotics, Mei and Choi (1987) deduced the equivalent strut width for a ship hull with a finite draft, and calculated the oscillatory forces on the ship due to the radiation of solitons. Recently, Chen and Sharma (1995) have improved the numerical scheme for solving the K-P equation and the accuracy of the ship hull boundary conditions. A sample result of their computation is shown in Figure 10 (from Chen and Sharma, 1995), showing the one-dimensional solitons radiated upstream and the two-dimensional waves downstream.

Besides engineering interests, the problem of upstream solitons has been studied in the oceanographic context. For example, interfacial waves in a two-layered sea can be induced by tides passing a topography. Nonlinear solitons can be expected to appear in a strait if a long topographical feature is

Figure 11.

Free surface evolution due to a ship advancing at the critical speed in a shallow channel. As time passes, more solitons are radiated upstream. (Chen and Sharma, 1995).

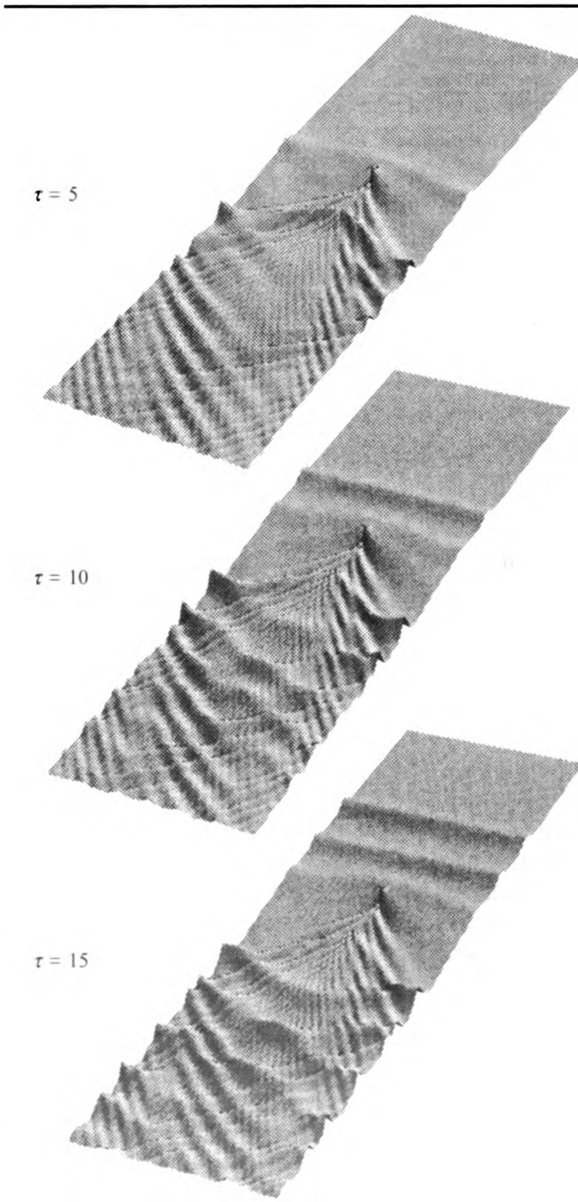

present either across the strait or along a coast (e.g., Melville and Helfrich, 1987). In a two-layered ocean two linear modes of internal waves with different phase speeds can exist. When the tidal flow speed is near either wave speed, upstream solitons are possible. For a continuously stratified sea, there can be many internal wave modes. Nonlinear dispersive effects near one of the critical wave speeds can be similarly complex and deserve further study.

Subharmonic resonance of articulated structures

The fabled city of Venice is situated in a small lagoon on the shore of the Adriatic Sea. Due to the dense population and industrialization, excessive use of groundwater has led to the lowering of land surface. Storm surges, which enter the lagoon through three inlets, now flood the city as often as 50 times per year. To save the ancient city from deterioration, engineers in Italy have proposed to construct a storm barrier across each of the three inlets (Bandarin, 1991). To allow tidal flushing of the lagoon and to preserve the scenic beauty, the barriers must be kept out of sight except during a storm. A design has been under consideration since 1984 for a barrier consisting of many steel boxes hinged on a common axis that is fixed on the seabed across each inlet. These boxes are unconnected with each other in order to reduce the cost for a strong support and for easy maintenance. When a storm is forthcoming, air is compressed into the boxes so that they rise to an inclination of 60 degrees from the horizontal. Because the inlet channels are long, the storm waves are expected to arrive with their crests parallel to the gates. Then the gates are expected to swing to and fro in unison, transmitting relatively little force and torque to the axis while serving as a dam to stop the ocean water from entering the lagoon.

Laboratory tests in Delft and in Italy have revealed an unexpected phenomenon, however. When the incident waves arrive at certain frequencies, the gates do not swing in unison. Instead, neighboring gates oscillate out of phase, therefore diminish the intended function as a dam. These laboratory tests also showed that the out-of-phase oscillations have frequencies just one-half of that of the incident waves.

Decades ago, subharmonic resonance was studied actively for an unrelated oceanographic phenomenon - surf beats that may contribute to the formation of beach cusps. They can also cause hazards in resonating harbors or for moored ships. It is known that along a sloping beach there can be natural modes called edge waves with energy trapped along the shore. Guza and Bowen (1976) showed that an edge wave can be excited subharmonically by normally incident wave. Theoretical analyses for steady incident waves were advanced by Rockliff (1978) and Miles (1990).

Mei, et al. (1994) found that the articulated construction of the Venice gates can support trapped waves that do not radiate energy to infinity. In fact, there can be a discrete set of modes where neighboring gates oscillate out of phase without radiating wave energy. They have tested the existence of one trapped mode by comparing the eigenfrequencies with experiments for two vertical gates in a narrow wave flume. Moreover, by sending normally incident waves at twice the eigenfrequency of a trapped mode (see Figure 11), resonance was produced. P. Sammarco has recently confirmed that the nonlinear behavior of the gate displacement B is governed by the Landau equation

$$-i\frac{\partial B}{\partial t} = \delta b + \alpha A B^{*} + \beta\, |B|^2 B\,, \tag{4.18}$$

where A is the incident wave amplitude. Mei and his colleagues P. Sammarco and H. Tran are now examining the stability, bifurcations and possible chaotic motions for periodically modulated incident waves with $A = A_o\,(1 + \mu \cos\Omega t)$, where Ω is a very small modulational frequency. An advance in modern science is finding its usage in a traditional engineering problem that dates back to 4000 BC, when Egyptians built the first breakwaters for the harbor of Alexandria.

Concluding Remarks

From the physical point of view, one of the most striking lessons learned in recent advances is that, given long enough time or large enough space, even weak nonlinearity can lead to significant changes to the linearized theories. Thus steady forcing can result in a transient response; deterministic input can yield a chaotic evolution. Many long-cherished concepts of linearized theories have fallen by the wayside. While nonlinearity is drawing attention in many scientific disciplines, the dynamics of ocean surface waves is still the most furtile ground for studying its impacts and finding more challenges.

From the viewpoint of theoretical analysis, efforts to gain new understandings have benefited significantly by the enhanced computer power in numerical simulation. It is, however, safe to predict that in the forseeable future analytical and numerical approaches will remain complementary for a long time; one cannot replace the other. The analytical approach is more effective when there are many different scales, especially for small amplitudes or weak nonlinearity. Numerical approaches are indisputably more powerful when dealing with finite amplitudes, but their power diminishes when many different scales and two or three dimensions must be considered. Future progress is likely dependent on the combination of the two approaches in some optimal way.

Acknowledgment

The author acknowledges with gratitude the sustained ONR support received since the beginning of his academic

career (Program of Fluid Mechanics, Program of Ocean Engineering, and The Accelerated Research Initiative on Nonlinear Ocean Waves). Partial support from the National Science Foundation for many years is also recorded with pleasure.

Biography

Chiang C. Mei is Edmund K. Turner Professor of Civil and Environmental Engineering at Massachusetts Institute of Technology. He received his PhD from Caltech in Engineering Science. After a two-year post-doctoral fellowship there, he moved to MIT, where he has remained ever since, except for a few sabbatical leaves. His research interests are: (i) ocean surface waves, including the fluid dynamical theory and applications in coastal and offshore engineering, (ii) dispersion of suspended particles near, and transport of cohesive fluid mud on, the seabed, (iii) dynamics of poroelastic media with applications to seabed mechanics and land subsidence, and (iv) diffusion and transport of volatile organic chemicals in porous media.

References

1. Ablowitz, M.J. & SegurR, H. (1981). *Solitons and the Inverse Scattering Transform*, Society Industrial and Applied Mathematics, Philadelphia.
2. Akylas, T.B. (1984). *J. Fluid Mech.* **141**: 455-466. Agnon, Y. & Mei, C.C. (1988). *J. Fluid Mech.* **195**: 201-222.
3.

Agmon, Y. & Mei, C. C. (1988) *J. Fluid Mech.* **195**: 201-222

4. Badulin, S.I., Pokazeyeu, K.V., & Rosenberg, A.D. (1983). *Izv. Atmos. Ocean. Phys.* **19** (10): 782-787.
5. Bandarin, F. 1991 *Coastal Zone 91*, Amer. Soc. Civ. Engrs. 3352-3370.
6. Battjes, J.A. (1988). *Annu. Rev. Fluid Mech.* **20**: 257-293.
7. Benjamin, T.B. & Feir, J.E. (1967). *J. Fluid Mech.* **27**: 417-430.
8. Bliven, L.F., Huang, N.E., & Long, S.R. (1986) *J. Fluid Mech.* **62**: 237-260.
9. Bowen, A.J. (1969). *J. Marine Res.* **27**: 206-214.
10. Brown, E.D., Buchsbaum, S.B., Hall, R.E., Penhune, J.P., Schmitt, K.F., Watson, K.M., & Wyatt, D.C. (1989). *J. Fluid Mech.* **204**: 263-293.
11. Carter, T.G., Liu, P.L.F., & Mei, C.C. (1973). *J. Waterways, Harbours Coastal Eng. Div. ASCE* **99**: 165-184
12. Chen, X. & Liu, Y. (1988). *Acta Mechanica Sinica*, **4** (3): 201-210.
13. Chen, X. & Sharma, S.D. (1995): *J. Fluid Mech.* **291**: 263-285.
14. Craik, A.D.D. (1985). *Wave Interactions and Fluid Flows.* Cambridge University Press.
15. Davies, A.G. & Heathershaw, A.D. (1984). *J. Fluid Mech.* **144**: 419-443.
16. Debnath, L. (1994). *Nonlinear Water Waves.* Academic Press.
17. Dysthe, K.B. (1979). *Proc. R. Soc. Lond.* **369**: 105-114.
18. Ertekin, R.C., Webster, W. C., & Wehausen, J. V. (1986) J Fluid Mech. **1659**: 275-292.
19. Feir, J.E. (1967). *Proc. R. Soc. London A* **299**: 54-58.
20. Fu, L.L. & Holt, B. (1982). *Jet Propulsion Lab. Publ.* 81-120.
21. Graff, W., Kracht, A., & Wwinblum, G. (1964). *Trans. Soc. Nav. Archit. Mar. Engnrs.* **72**: 374-401. Gu, D. F. & Phillips, O.M. (1995). *J. Fluid Mech.* **275**, 301-321.
22. Guza, R.T. & Bowen, A.J. (1976). *J. Marine Res.* **34**: 269-293.
23. Hammack, J., Scheffner, N., & Segur, H. (1989). *J. Fluid Mech.* **209**, 567-589.
24. Hara, T. & Mei, C.C. (1987). *. Fluid Mech.* **178**: 221-241.
25. Hara, T. & Mei, C.C. (1991). *J. Fluid Mech.* **230**: 429-477.
26. Hara, T. & Mei, C.C. (1994). *J. Fluid Mech.* **267**: 221-250.
27. Harrison, W.J. (1909). *Proc. Lond. Math. Soc.* **7**: 107-121.
28. Heathershaw, A.D. (1982). *Nature* **296**: 343-345.
29. Henyey, F.S., Creamer, D.B., Dysthe, K.B., Schulz, R.L., & Wright, J.A. (1988). *J. Fluid Mech.* **189**: 443-462.
30. Huang, D.B., Sibul, O.J., Webster, W.C., Wehausen, J.V., Wu, D.M., & Wu, T.Y. (1982). *Proc Conf. on Behavior of Ships in Restricted Waters*, Varna, Bulgaria, 26.1-26.9.
31. Izubuchi, T. & Nagasawa, S. (1937). *Jap. Soc. Nav. Archit.* **61**, 165-206.
32. Kinoshita, M. (1946). *Jap. Soc. Nav. Archit.* **76** 174-213.
33. Koman, G.J., Cavaleri, L., Donelan, M., Hasselmann, K., Hasselmann, S., & Janssen, P.A.E. (1995)/ *Dynamics and Modelling of Ocean Waves.* Cambridge University Press.
34. Lake, B.M., Yuen, H.C., Rungaldier, H., & Ferguson, Jr., I.N.E. (1977). *J. Fluid Mech.* **83**: 49-74.
35. Lea, G.K. & Feldman, J.P. (1972). *Proc. 8th Suymp. Naval Hydrod* Paris, 1527-1651.
36. Lighthill, M.J. (1967) *J Fluid Mech.* **27**: 725-752.
37. Liu, P.L.-F. (1989). *J. Fluid Mech.* **205**: 163-170.
38. Liu, P. L-F. (1994) *Advances in Coastal and Ocean Engineering*, I, World Scientific. 125-158.
39. Lo, E. & Mei, C.C. (1985). *J. Fluid Mech.* **150**: 395-416.
40. Longuet-Higgins, M.S. (1970a,b). *J. Geophys. Res.* **75**: 778-6789; 6790-6801.
41. Longuet-Higgins, M.S. (1987). *J. Fluid Mech.* **177**: 293-306.

42. Longuet-Higgins, M.S. & Stewart, R.W. (1960). *J. Fluid Mech.* **8**: 565-583.

43. Maruo, H. (1948). *Jap. Soc. Nav. Archit.* **84** (1952): 1-15.

44. Maruo, H. & Tachibana, T. (1981). *Jap. Soc. Nav. Archit.* **150**: 181-187.

45. McGoldrick, L.F. (1965). *J. Fluid Mech.* **21**: 305-331.

46. Mei, C.C. (1985). *J. Fluid Mech.* **152**: 315-335.

47. Mei, C.C. (1986). *J. Fluid Mech.* **162**: 53-67.

48. Mei, C.C. (1989). *The Applied Dynamics of Ocean Surface Wave*. World Scientific.

49. Mei, C.C. & Agnon, Y. (1989). *J. Fluid Mech.* **208**: 595-608.

50. Mei, C.C. & Benmoussa, C. (1984). *J. Fluid Mech.* **139**: 219-235.

51. Mei, C.C. & Choi, H.S. (1987). *J. Fluid Mech.* **179**: 59-76.

52. Mei, C.C. & Liu, P.L.-F (1993). *Annu. Rev. Fluid Mech.* **25**: 215-240.

53. Mei, C.C. & Naciri, M. (1991). *Proc. R. Soc. Lond. A* **432**: 535-546.

54. Mei, C.C., Sammarco, P., Chan, E.S., & Procaccini, C. (1994). *Proc R. Soc. Lond.* **444**: 257-265.

55. Melville, W.K. (1982). *J. Fluid Mech.* **115**: 165-185.

56. Melville, W.K. & Helfrich, K.R. (1987). *J. Fluid Mech.* **178**: 31-52.

57. Melville, W.K. & Rapp, R.J. (1988). *J. Fluiud Mech.* **189**: 1-22.

58. Miles, J.W. (1977). *J. Fluid Mech.* **79**: 171-179.

59. Miles, J.W. (1990). *J. Fluid Mech.* **214**: 43-57. Molin, B. (1982). *Pap. Ship Res. Inst.*, Tokyo, Japan 68.

60. Munk, W.H., Scully-Power, P. & Zacheriasen, F. (1987). *Proc. R. Soc. Lond. A.* **412**: 231-254.

61. Naciri, M. & Mei, C.C. (1992). *J. Fluid Mech.* **235**: 415-452.

62. Naciri, M. & Mei, C.C. (1994). *Wave Motion.* **20**: 211-232.

63. Okamura, M. (1995). *Wave Motion.*

64. Phillips, O.M. (1960). *J. Fluid Mech.* **9**: 193-217.

65. Phillips, O. M. (1978) *The Dynamics of the Upper Ocean*, Cambridge University Press.

66. Phillips, O.M. (1981). *J. Fluid Mech.* **107**: 465-485.

67. Pokazeyeu, K.V. & Rosenberg, A.D. (1983). *Oceanologiya* **123**: 429-435.

68. Rockliff, N. (1978). *Math. Proc. Cambridge Phil. Soc.* **83**: 463-479.

69. Shemdin, O.H. (1990). *J. Geophys. Res.* **95**: c9. 16319-16338.

70. Shyu, J.H. & Phillips, O.M. (1992). *J. Fluid Mech.* **217**: 115-141.

71. Su, C.L. (1973). *J. Waterways Harbor Coastal Eng. Div.* ASCE 375-391.

72. Thews, J.G. & Landweber, L. (1935). *U.S. Expr. Model Basin Report 408*, Navy Yard, Washington, D.C.

73. Trulsen, K. & Dysthe, K.B. (1990). *Water Wave Kinematics* A.Torum, Ol.,T. Gudmestad (eds.) Kluwer Academic.

74. Trulsen, K. & Dysthe, K.B. (1992). in *Breaking Waves*, IUTAM Symposium in Sydney/Australia 1991, M.L. Banner, R.H.J. Grimshaw (Eds.), Springer-Verlag Berlin Heidelberg.

75. Trulsen, K. & Mei, C.C. (1993). *J. Fluid Mech.* **251**: 239-271.

76. Trulsen, K. & Mei, C.C. (1995). *J. Fluid Mech.* **290**: 345-376.

77. Tulin, M. & Miloh, T. (1990). *Proc. 18th Symp. Naval Hydrod., Ann Arbor.* Ursell, F. (1953). *Proc Cambridge Phlos. Soc.* **49**: 685-694.

78. Wilton, J.R. (1915). *Phil. Mag.* **29**: 688-700.

79. Wu, T.Y. (1987). *J. Fluid Mech.* **184**: 75-99.

80. Wu, J.-K. & Liu, P.L.-F. (1990). *J. Fluid Mech.* **217**: 595-613.

81. Wu, D.M. & Wu, T.Y. (1982). *Proc. 14th Symp. Naval Hydrod., Ann Arbor*, 103-129.

82. Yuen, H.C. & Lake, B.M. (1980). *Ann. Rev. Fluid Mech.* **12**: 303-334.

83. Zabusky, N.J. & Kruskal, M.D. (1965). *Phy. Rev. Lett.* **15**: 240.

84. Zhang, J. & Melville, W.K. (1990). *J. Fluid Mech.* **214**: 321-346.

85. Zhou, C. & Liu, P.L.-F. (1987). *J. Fluid Mech.* **175**: 143-155.

What Can We Learn from Wave Tank Experiments?

Norden E. Huang and Steven R. Long
NASA Goddard Space Flight Center
Laboratory for Hydrospheric Processes / Ocean and Ice Branch
Greenbelt, MD

Abstract

Wave tank experiments have provided the indispensable data for the past advances in the studies of nonlinear dynamics of the ocean waves. Experimental results on nonlinear wave-wave interactions and wave instabilities, wave breakings, wave statistics, wave induced longshore currents, wave blockings and trapping when encounter currents, and wave observation under nonstationary conditions all showed the importance of the laboratory observations. In most of the cases, field observation just cannot provide detailed enough data for us to understand the physics of the phenomena. Thus, laboratory experiments are not only indispensable, but also the most cost-effective way to study the nonlinear ocean wave phenomena.

Introduction

Wave motion was among the first natural phenomena studied mathematically by scientists. The giants in mathematics and theoretical mechanics such as Lagrange, Airy, Stokes, Laplace, Russel, and Rayleigh have all left their marks in this field. Past studies, however, have been centered on the infinitesimal undulation of the water surface with harmonic distortions. New and deeper understanding of wave dynamics only started with the discoveries of weak nonlinear wave-wave interactions that describe the longer term wave evolution. With few exceptions, most of the theoretical advancements made were inspired by direction observations with the laboratory observations constituting most of the success. These observations provided not only confirmations of the existing theories, but also new insights and inspirations for further developments. The field observations, though indispensable for final confirmation of the theory for applications, will probably never play as crucial a role as the laboratory in advancing the fundamental understanding of wave dynamics.

Being motions confined to the air-water interface with a huge density difference between the air and the water, even the highly nonlinear wave motions are amenable to the inviscid approximation. Consequently, an irrotational motion can offer an accurate depiction of the phenomenon. Because of these properties, the laboratory experiments can provide good simulations for us to study most of the controlling mechanisms of the wave dynamics. Nevertheless, as close as the laboratory results can be to those of the natural phenomena, a laboratory experiment still cannot fully simulate the complicated balance of different natural forces. Therefore, in designing an experiment, one should know what mechanism to simulate, what forces need to be controlled and monitored, before mounting the tests. Through careful planning, detailed measurements under controlled conditions can yield enough data for comparisons with the theory, and for reaching statistically significant

Figure 1.

Resonant wave interaction measured by McGoldrick et al. (1966). Wave with frequencies f_1 and f_2 were generated mechanically. According to Phillips (1960) theory, resonance will occur when f_1/f_2=1.775, at the frequency $2f_1$-f_2. The two spectra measured in a wave tank showed the resonant interaction at work.

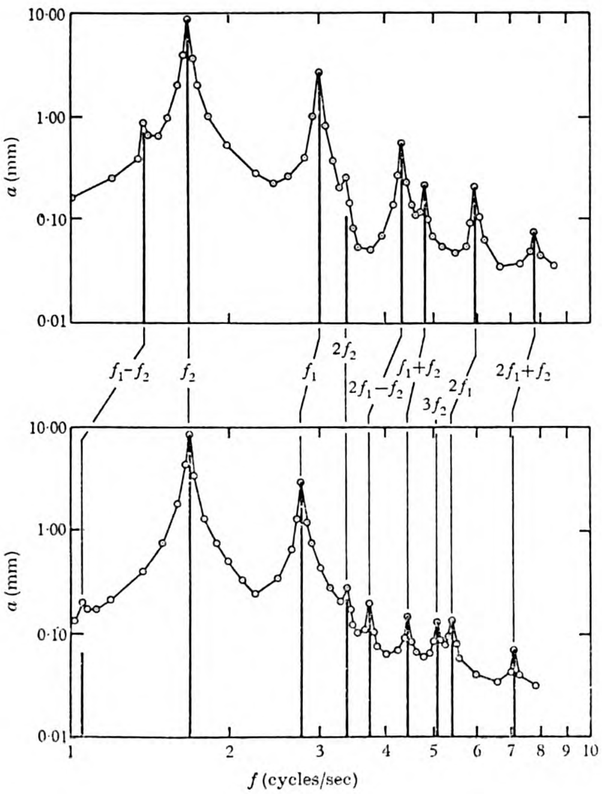

conclusions. Additionally, laboratory experiments are extremely attractive in the present limited budgetary period, for an experiment can be completed with a minimum amount of expense comparing to the full field tests. In the following sections, we will give a few examples of the wave properties we have learned from the laboratory experiments, and the insight gained from such observations.

Laboratory Experiments

Nonlinear Wave-Wave Interactions and Instability

The starting point of modern water wave theory can be placed rightfully at the discovery of the weakly resonant nonlinear wave-wave interactions by Phillips (1960). Later, Lighthill (1965, 1967) pointed out that a deep water wave train can be unstable. Phillips (1967) identified the instability as a consequence of the nonlinear resonant interactions. The nonlinear interaction and the wave instability thus became the central problem for the deep water wave studies. Laboratory experiments by McGoldrick, *et al.* (1966) and Longuet-Higgins and Smith (1966) provided quantitative evidence of these interactions as shown in Figure 1. The theoretical and experimental observations by Benjamin and Feir (1967) and Benjamin (1967) have provided conclusive proof of the instability, as well as demonstrate how theory and experiment can cooperate to advance our knowledge into new territory. Indeed most of the salient properties of the wave evolution such as the instability and the frequency down shift (Hasselmann, 1962) were all observed in laboratory settings (Lake *et al.* , 1977; Lake and Yuen, 1978; Yuen and Lake, 1982; and Huang *et al.*, 1986). These basic ideas are responsible for the nonlinear source function, the key part in the third generation wind-wave prediction model (Komen, *et al*, 1994).

Following these pioneering studies, Su (1982 a, b), Su *et al.* (1982), and Su and Green (1984) have also observed higher order resonant interactions in the laboratory that involve five waves, resulting in the three-dimensional instability, as shown in Figure 2. These observational results have inspired the theoretical analysis of the higher order resonant interaction by McLean (1982 a, b). The theoretical and experimental observations have defined the pattern of wave evolution to a high degree of accuracy.

Even with these successes, the details of the frequency downshift is still unknown: Is it a continuous process as assumed in the classic treatment? Or is it a discrete process as observed by Lake and Yuen (1978) and Ramamonjiarisoa and Mollo-Christensen (1979)? The puzzle was further investigated by Huang (1995) and Huang *et al.* (1996), who proposed

Figure 2.

Three dimensional wave pattern generated at an outdoor wave channel by Su (1982). The initial waves are two dimensional.

Figure 3.

Wave elevation data measured in the laboratory with the wave maker set at 2.5 Hz, and an initial steepness at 0.2. The vertical axis indicates the distance from the wave maker. Notice the increasing modulation of the wave envelope as the waves evolve.

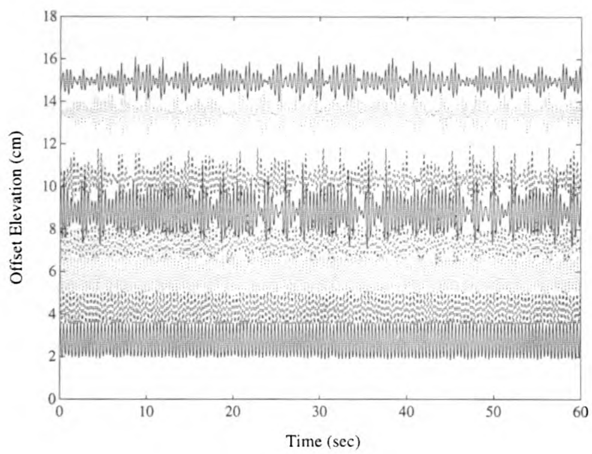

that the wave evolutionary processes were actually *local*, and *abrupt*. These conclusions were based on the analysis of data again from the laboratory by a pioneering new the Characteristic Scale Decomposition Method, which was then linked to their Hilbert Spectrum Analysis. This approach provides the local amplitudes and instantaneous frequencies that are finally used to produce a joint distribution that can be contoured as a time-frequency distribution. As shown by Huang *et al.* (1996), the Hilbert Spectrum produced a vastly better resolution in both time and frequency localization than the wavelet analysis.

Let us examine the processes of frequency downshift in more details. Following Huang *et al.* (1996), who studied the phase changes starting from a uniform reference state. They showed that the wave frequency downshift was achieved through a local process: Two waves combine and become one, or three waves combine and become two. In general, n waves would combine to become (n - 1) waves. Other than the waves involved actively in these local processes, all the other waves are left unaffected. Each time, one and only one wave would disappear locally within the time span of only one wave period. The process is designed by Huang *et al.* (1996) as the 'fusion.' In the initial two-to-one stage, it is identical to the 'lost crest,' the 'crest pairing' and the 'phase reversal' idea reported before by others, but the subsequent observed variations were more general. They showed the process quantitatively through the phase function.

The details of the wave fusion process are illustrated by the following laboratory data set. Figure 3 shows the original wave elevation data as used in Huang (1995) and Huang *et al.* (1996), with wave maker frequency of 2.5 Hz and the initial steepness set at 0.20. This gives an overall view of all the measurement locations, in which the vertical axis indicates the distance from the wave maker. The wave elevation data show that the waves at the shortest fetch (about 3 m) are quite uniform, but already have slight amplitude modulations. As the waves evolve, the amplitude modulations grow with the fetch. If one uses the Fourier spectral analysis to examine the frequency variations, he will only see the sideband growth, and, eventually, the lower lobe of the sideband overtakes the main peak to become the most energetic peak at station 8 (for a fetch at 8 m).

The process of the frequency downshift was further examined with the Hilbert Transform as in Huang *et al.* (1996). After applying the Hilbert transform to all the data, the unwrapped phase is plotted in Figure 4. Because the overall slope of the phase function should be the mean frequency, the decrease in the overall slope of the phase function thus indicates a decrease of the mean frequency. At this scale, the trend seems to suggest a global, gradual and continuous change of the phase function or frequency. The slope of the first four stations, in fact, stays almost identical to that of the first station. The first time the phase function shows any deviation from this initially closely clustered group is station 5, but even this change in the phase seems only to be able to give a small and gradual change in frequency.

Huang *et al.* (1996) examined the phase changes by taking the difference of the phase functions of all stations with respect to that of the first station as the reference state. The difference is shown in Figure 5. From this figure, we can see that the changes of the phase functions consist of a series of steps with the sharp jumps confined in very short time spans. Thus, in seemingly stationary data, we find local transient phenomena. To have a quantitative assessment of the phase anomalies, they introduced the phase-amplitude diagram, a method new to water waves, which is a plot of the amplitude envelope as a function of the phase difference between the local values and that of the reference state. A typical result is shown in Figure 6 for station 5.

A section of the time series wave elevation data from station 5 is expanded and displayed in Figure 7 a and b in a two-way comparison. When the data from station 5 are superimposed on its phase difference from station 1, the time domain associated with the jump in phase values could be easily confined within a single wave. Then the raw elevation data from station 5 are superimposed on those from station 1 as shown in Figure 7 b. All the wave peaks obviously line up except at the location of the phase jump, where two waves fuse into one. Thus, in the time span of two waves seen at station 1, now it contains only one wave locally at station 5. The period

Figure 4.

Unwrap phase for all the stations as shown in Figure 3. At this scale, the change of phase values seems gradual and global.

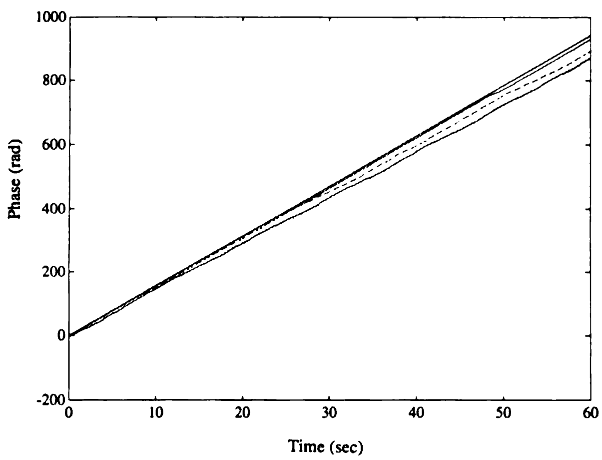

is doubled; the local frequency is, therefore, one half of the reference state. This local change in frequency also indicates group velocity change as reported by Melville (1983). These results have provided a quantitative measure to the qualitative observations by Lake and Yuen (1978), Ramamonjiarisoa and Mollo-Christensen (1979); they have also removed the uncertainty expressed by Melville (1983) on whether the period indeed doubled at the 'crest pairing.' The 'crest pairing' is clearly demonstrated as a combination of two waves, where the phase loss is precisely 2.

Huang *et al.* (1996) have further concluded that the phase jumps shown here are cumulative, counting relative to the base of the reference state. On careful examination, one can see two types of phase jumps: (1.) The simple one involving two waves fusing into one; and the complex one involving n waves fusing into (n - 1) waves. The changes are local. Both characteristics are drastic departures from the traditional view of the wave motions: Other than the limited time duration where fusion is underway, the mean frequency remains unchanged from the initial state. The fusion region expands discretely and locally, and eventually covers the whole time axis. Each fusion event can be either a 'crest pairing' or a 'trough pairing.' The frequency downshift is an accumulated effect of fusions of two or more waves and a readjustment of local frequency. These processes are irreversible. This asymmetry is due to the preferred direction of downward energy flow. These results also raise concerns about the past assumptions on slowly varying wave trains. These problems clearly need to be resolved theoretically; we need a new paradigm for wave study. Wave tank experiments have made a significant contribution to this so far, and the wave tank will continue to make significant contribution in the future.

Wave Breaking

Wave breaking is the key in determining the wave energy dissipation, the turbulence generation in the upper ocean layer, the formation of the mixed layer, and the fluxes of energy and momentum across the air-sea interface. In fact, it can be linked to all the upper ocean layer dynamic phenomena as suggested by Huang (1986). Although great advances have been made in the last twenty years, progress in the study of breaking waves have been painfully slow. Our state-of-the-art understanding of breaking has recently been reviewed by Banner and Peregrine (1993). It is a difficult problem to treat analytically and experimentally; the fundamental problems on breaking wave studies are still left unresolved: Of which the foremost is a precise definition of wave breaking. This seemingly obvious problem assumes a very different form in the wideband random sea, where breaking involves not only the obvious whitecaps generating events, but also the countless not so obvious microscale breakers. Granted, it is widely accepted that a breaking event occurs when the velocity of a water particle near the surface exceeds the wave phase velocity. Still, there are so many velocity scales in a wideband wave field. The issue is further complicated by the fact that the surface velocity in the field is difficult to measure, while the only measurement of the surface velocity is again performed in the laboratory. Without a precise definition has hampered the measurements. As a result, optical detection of whitecaps, wave gauge detec-

Figure 5.

The phase function deviations from a reference state chosen as station 1. Notice the localized jumps of the phase functions at this scale. The amount of phase jumps are all 2π.

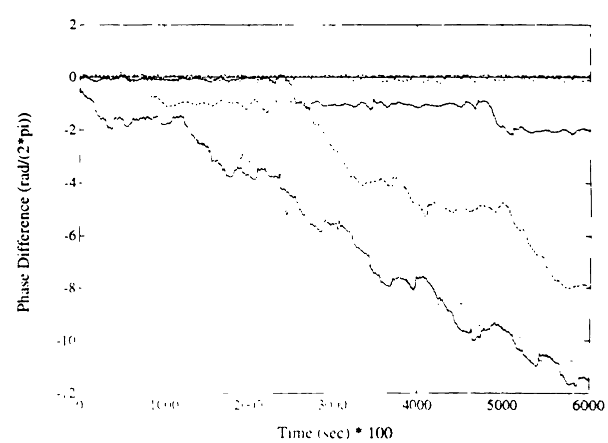

Figure 6.

The phases-amplitude diagram for station 5. Notice the discrete jumps in phase values.

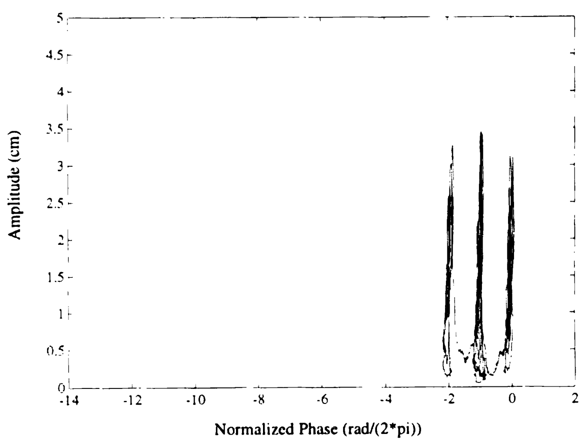

Figure 7.

Detailed comparisons for a selected section of data at station 5.
(a) Raw data superimposed on the corresponding phase function for the same time period. The time span covering the phase jump is confined within one wave period near the 49th second.
(b) The same ra data superimposed on the data from station 1 serving as a time scale here. The wave near the 49th second shows a clear 2-to-1 simple fusion event.

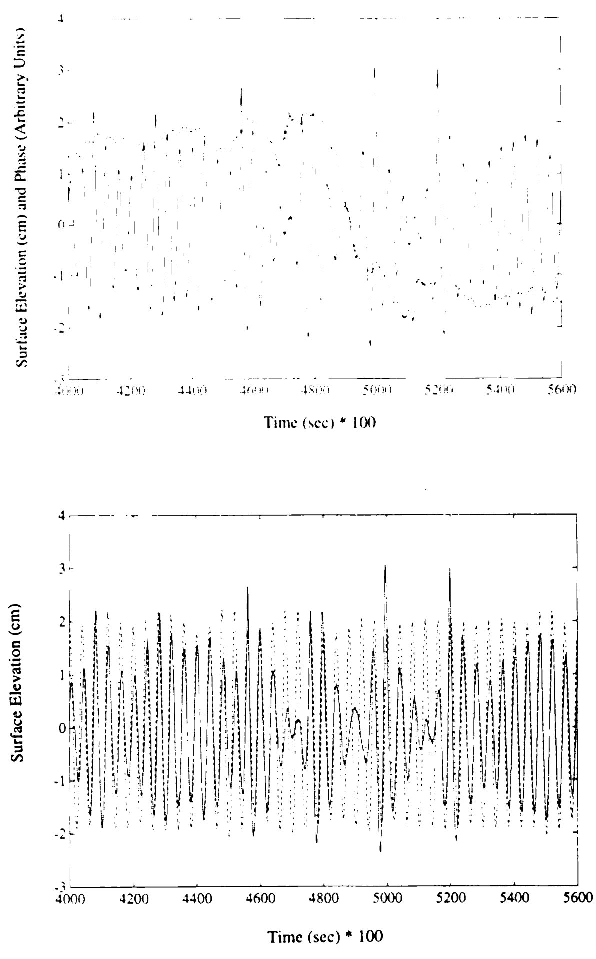

tion of surface elevation jumps, radar detections of large Doppler frequency shift or large reflection spikes, and acoustic detection of noise generated by the bubbles generated by the breakers have all been used as surrogates for breaking with mixed results. Really quantitative measurements are actually taken place in the laboratory.

Most of the laboratory breaking waves are generated mostly by the following ways: The first is in a steady flow with a submerged stationary hydrofoil as did by Banner and Melville (1976), Banner and Fooks (1985), and Banner (1990). A variation of this method is to tow a submerged hydrofoil in standing water as did by Duncan (1981, 1983). These studies established that the breaking wave can indeed increase radar reflectivity, generate underwater noise, enhance the momentum flux. The details of the breaking wave measurements also enabled Cointe (1987) to publish a theory of the dynamic of steady breaking waves, and established a numerical model. The second method is to generate breaking waves by focus waves in a preselected point as reported by Rapp and Melville (1990). Among the most significant findings is the great efficiency of breaking waves in transferring momentum and energy from wave field to the water column. They have also measured the surface motion, momentum flux, energy loss due to breaking, breaking induced surface currents, turbulence generation, and mixing. These results constitute the most comprehensive body of our knowledge concerning the breaking waves so far.

On the theoretical side, Longuet-Higgins (1982, 1986), in a brilliant display of his analytic prowess, has found analytic solutions for overturning fluid motions. He showed that the tip of an overturning breaking waves can be model by a slender hyperbola. For a plunging breaker, the shape of the forward face can be modeled by a simple parametric cubic curve as in Figure 8. Such agreement between laboratory data and theoretical results is indeed encouraging. Even with these remarkable successes, the difficult problem of understanding the true three dimensional breaking of the natural wind waves in field

Figure 8.

The comparison between a laboratory plunging breaker front profile with the cubic parametric curve proposed by Longuet-Higgins (1986).

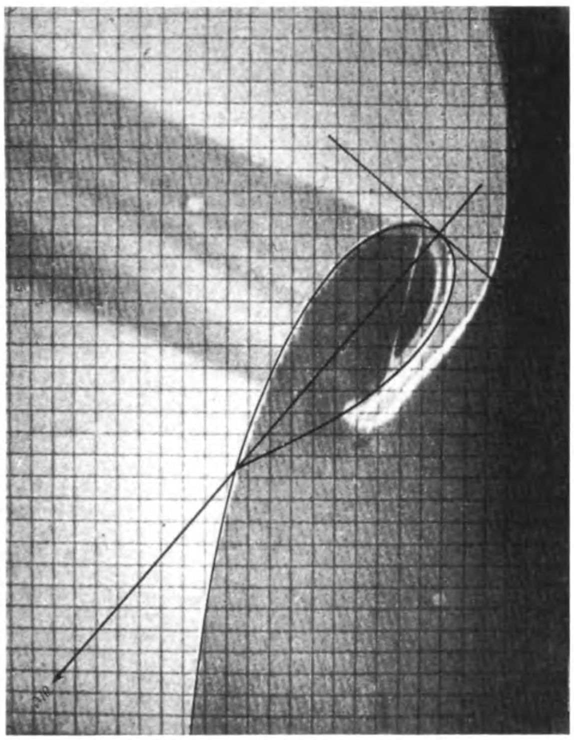

is still a formidable challenge. Our present knowledge concerning those events amounts only a theoretical model by Phillips (1985), and some detailed laboratory observation of the breaking wave kinematics by Bonmarin (1989). More quantitative data are needed for further advance our knowledge.

Wave Statistics

Wave statistics is important for engineering design, remote sensing, and for understanding the dynamics of the random wave field. Studies of the wave statistics are made difficult by the lack of data. Through theoretical analysis (Longuet-Higgins, 1963), it was found that the nonlinear effect can make the surface elevation distribution non-Gaussian. From laboratory data, Huang and Long (1980) demonstrated the agreement between theoretical result and actual measurements, as shown in Figure 9. This demonstrated that nonlinear analysis based on perturbation of potential motion of waves can work very well sometimes. This work was later extended by Huang *et al*. (1984) to demonstrate that the joint probability density function of slope and elevation was also non-Gaussian, giving a further example of how theoretical development and laboratory verifications can work together to advance knowledge as in Figure 11. Encouraging as these earlier results were, they were still limited to narrow band cases, with building blocks of the theory resting on the Stokes wave. But the approach did give insight into the local statistical properties and the dominant mechanism, instantaneous modifications of the wave profile resulting in crest-trough asymmetry. Laboratory data were also used to determine the key parameters in a wave spectral model as discussed by Huang *et al* (1990 a and b).

Wave Induced Longshore Currents

Longshore current is an important phenomenon in the littoral zone. Traditionally, the generation mechanism has been identified as the breaking waves (see, for example, Longuet-Higgins, 1970 a and b). This mechanism is an important one. Neglected, however, is the role played by the non-breaking oblique long waves at the coastline, which has been shown by Zhang and Wu (1996) to be also important in generating the longshore current. Surface gravity waves, generated by wind either over the local region or at a great distance, can produce surf beats and drive the waves up on the beach. At an oblique incidence angle, the excess momentum can generate strong longshore currents even without breaking. To solve this problem, one must consider the three-dimensional run-up of long waves on a beach with sloped bottom. The plane problems of run-up and reflection of waves incident normally on a sloping beach have been investigated by Carrier and Greenspan

Figure 9.

Laboratory measurement of the probability density function for wind waves compared with the theory of Longuet-Higgins (1963) (smooth line) and the eight term Edgworth Expansion (dotted line).

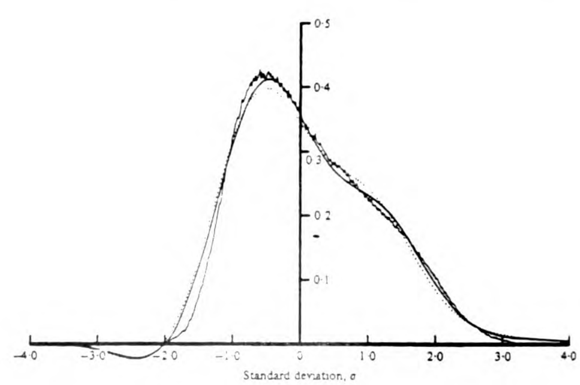

Figure 10.

Contour and prospective views of the joint probability density function for slope and elevation for a significant slope of 0.0323.

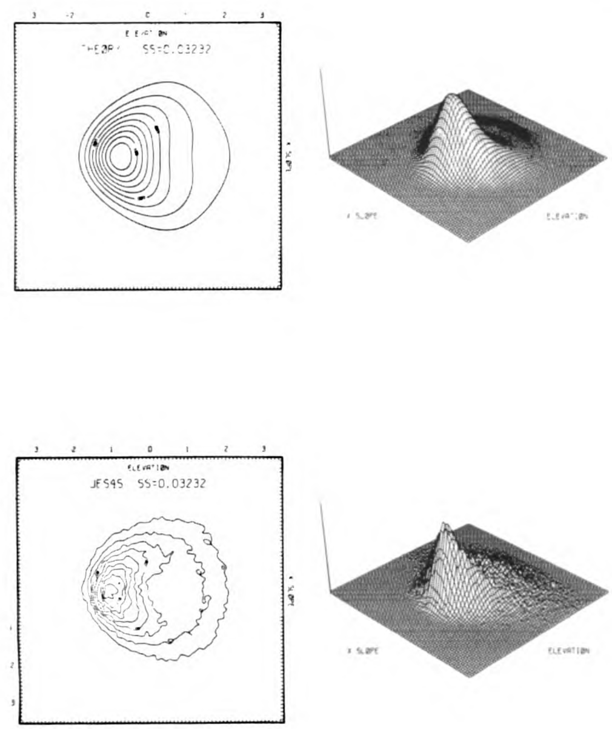

Figure 11.

Six consecutive top views of the longshore current generated by a train of obliquely incident cnoidal wave train with frequency at 1.23 Hz, at an angle of 29° to the coastal line. The beach is sloped at 7°. The six panels represent different time after the release of the dye: (1) t=0; (2) t=15 sec; (3) t=28 sec; (4) t=45 sec; (5) t=66 sec; and (6) t=97 sec. The speed can be inferred by the movement of the dye streak over the bottom grid at 2X2 cm.

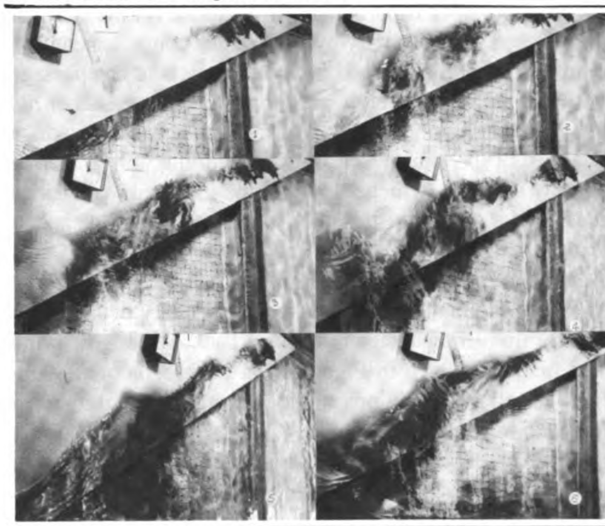

(1958), Carrier (1966), and Tuck and Hwang (1972) based on Airy's model. Numerical calculations have been tried by Kim *et al.* (1983) based on the Euler model. For the case of three-dimensional coastal dynamics, Carrier and Noiseux (1983) evaluated the oblique run-up and reflection of long waves on a plane beach based on linear wave theory. New results of oblique run-up, refraction and reflection over an arbitrary variable down slope were obtained by Zhang and Wu (1996) based on the same method as used by Teng and Wu (1992, 1994) to the wave propagation in a channel of arbitrary shape. Most remarkably, the closed form solution of the wave induced mass transport near the coast without breaking has a magnitude comparable to that generated by the breaking ones especially at the water line. To sort out the details of the mechanism, a laboratory experiment was conducted at California Institute of Technology by them. A typical result is given in Figure 12 in which the dye streaks vividly demonstrated the strength of the circulation set up by the oblique incident waves. The magnitude of the current agrees well with the theoretical predicted value. Unlike the breaking induced longshore current, this new model predicts the wave induced current to cover the whole nearshore zone. Recent field observation at Duck using tower-mounted video also indicated that the wave to current energy conversion process was not localized at the breaking point, but covered a considerable distance shoreward (Long and Sallenger, 1995). Thus, laboratory experiments again provided a demonstration of the mechanism for the important problem of long-shore current generation. This discovery is important for coastal circulation modeling, for it provides the boundary condition for the current field. In view of the importance assigned to the long ignored coastal zone dynamics, this phenomenon deserves careful further evaluation in the future.

Wave Blocking and Trapping

The blocking and trapping of wave packets by inhomogeneous flow fields again have been studied in a laboratory setting by Lai *et al* (1989) and Long *et al.* (1993). Evidence of multiple reflections and thus trapping within the current gradient zone near the blocking point has also been reported by Pokazeyev and Rozenberg (1983). A strong current gradient zone near the blocking point was seen to trap wave energy, shifting the wave numbers into the capillary range as shown in Figure 12. The production of capillary waves by this mechanism is in the range of the microwave wavelength of many remote sensors, and can explain why SAR can image the bottom bathymetry, though the electromagnetic wave pulse of the remote sensor could not really penetrate the water surface to any extent. When local current gradients are related to bottom features, then trapped waves can be found in patterns related to the bottom topography, and thus detected remotely.

Nonstationary Wave Observations by Ensemble Averaging

The laboratory is particularly well suited for the study of transient and nonstationary events. Under computer control, events such as the collision of two wave packets, the passage of a wave packet through a wind-wave field (see Chu *et al.*, 1992), and the initialization of surface roughness by sudden wind gusts (Spedding *et al.*, 1992; Spedding, 1996) can be precisely repeated, which allows all the identical realizations necessary for good statistics to be studied by means of ensemble averaging techniques. As shown in Chu *et al.* (1992), this ensemble averaging of 100 realizations led to the discovery of some new phenomena, the overshoot of energy density as it recovers from the passage of a wave packet through a wind wave field, as shown in Figure 13. This overshoot was observed for all the conditions studied. In the surface roughness initialization study by Spedding (1996), the laboratory again provided the detailed quantitative data that would be almost impossible to collect in the field. Experiments like this can be conducted in a computer controlled laboratory as described by Long (1992). Such data can provide truly ensemble average of complicated nonstationary or transient phenomena. Thus, laboratory is posed to make another fundamental contribution in the air-sea interface dynamics.

Conclusion

All the above experiments have shown that wave tank experiments can indeed play a significant role in understanding not only wave dynamics but also the associated dynamic phenomena. Such experiments can work with theoretical efforts to insure a real-world connection between theoretical developments and measurable phenomena. It is the classical cause and effect relationship in action: theoretical efforts can examine the cause and predict the effect, while experimental methods can verify the predicted effect, and even suggest alternate causes. This can confirm theory, or reveal reasons for its revision or expansion along another path. To date, most significant wave related dynamic phenomena were first found in the laboratory. Therefore, the laboratory studies are indispensable means for water wave investigations.

Wave tank experiments are also extremely cost-effective. Computer controlled facilities are available now for studying the most complicated nonstationary and transient wave phenomena. In the present tight budget situation, laboratory study should be seriously considered as an alternative.

Acknowledgments

The authors have been supported in the past by various ONR Programs that include the Physical Oceanography, the Fluid Mechanics, the Coastal Process, and the Physics Programs, without which many of the experiments could not

Figure 12.

A typical case of non-breaking blocking of waves by opposing current. The waves propagates from left to right encounter a current of 30 cm/sec. The waves are stopped without breaking. Capillary waves can radiate beyond the blockage point as indicated by the fine wave pattern reflection on the back wall.

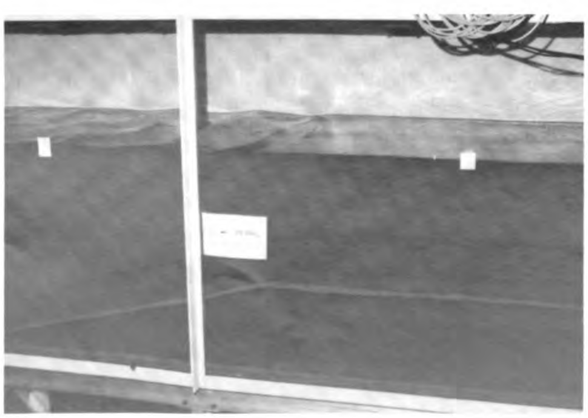

Figure 13.

The mean-square surface displacement of short wind-waves passing a fixed elevation probe. The is the ensemble average of 100 realizations, with the ensemble average of the longer wave packet removed. The wave packet passes this location between the 8 and 14 second mark.

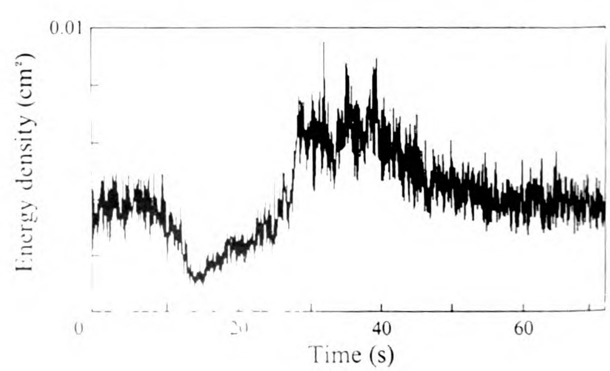

have been possible. In fact, NEH was supported by an ONR grant when he was a graduate student more than thirty years ago. This study has also been supported by NASA RTOP program in Oceanic Processes.

Biographies

Norden E. Huang received his B.S. in Civil Engineering from National Taiwan University in 1960, and Ph.D. in Fluid Mechanics from the Johns Hopkins University in 1967. During his graduate study at Hopkins, he was supported by an ONR grant to investigate the nonlinear wave-wave interactions problem. After almost six years of teaching at N.C. State University, he joined the National Aeronautics and Space Association (NASA) as a research scientist. Throughout the last ten years, he has been supported by Fluid Mechanics, Physical Oceanography, and Coastal Programs at ONR to study various problems of wave-current interactions and nonlinear wave evolution problems. Other than the wave studies, he has worked on the methods for non-stationary and nonlinear data analysis.

Steve R. Long received his B.S. and M.S. in Physics, and his Ph.D. in Oceanography from N.C. State University in 1975. He began his career with NASA as a research associate with the National Research Council. He has produced publications in professional journals and books, as well as presentations at national and interntional meetings. He also schedules and manages the NASA Air-Sea Interaction Research Facility at Goddard Space Flight Center/Wallops Flight Facility. He is a member of the American Meteorological Society and the American Geophysical Union.

References

1. Banner, M. L. (1990). Influence of wave breaking on the surface pressure distribution in wind wave interactions. *J. Fluid Mech.*, 211, 463-495.
2. Banner, M. L. and E. H. Fooks (1985). On the microwave reflectivity of small-scale breaking water waves. *Proc. Roy. Soc. Lond.*, A399, 93-109.
3. Banner, M. L. and W. K. Melville (1976). On the separation of air flow over water waves. *J. Fluid Mech.*, 77, 825-842.
4. Banner, M. L. and D. H. peregrine (1993). Wave breaking in deep water. *Annu. Rev. Fluid Mech.*, 25, 373-397.
5. Benjamin (1967). Instability of periodic wave trains in nonlinear dispersive systems, *Proc. Roy. Soc. Lond.*, A299, 59-75.
6. Benjamin, T. B., and J. E. Feir (1967). The disintegration of wave trains on deep water. I. Theory., *J. Fluid Mech.*, 27, 417-430.
7. Bonmarin, P. (1989). Geometric properties of deep-water breaking waves. *J. Fluid Mech.*, 209, 405-433.
8. Carrier, G. F. and Greenspan, H. P. (1958). Water waves of finite amplitude on a sloping beach. *J. Fluid Mech.*, 4, 97-109.
9. Carrier , G. F. (1966). Gravity waves on water of variable depth. *J. Fluid Mech.*, 24, 641-659.
10. Carrier, G. F. and Noiseux, C. F. (1983). The reflection of obliquely incident tsunamis. *J. Fluid Mech.*, 133, 147-160.
11. Chu, J. S., S. r. Long, and O. M. Phillips (1992). Measurements of the interaction of wave groups with shorter wind-generated waves. *J. Fluid Mech.*, 245, 191-210.
12. Cointe, R. (1987). *A theory of breakers and breaking waves.* PhD dissertation, University of California, Santa Barbara.
13. Duncan, M. A. (1981). An experimantal investigation of breaking waves produced by a towed hydrofoil. *Proc. Roy. Soc. Lond.*, A377, 331-348.
14. Duncan, M. A. (1987). The breaking and non-breaking wave resistance of a two-dimensional hydrofoil. *J. Fluid Mech.*, 126, 507-520.
15. Hasselmann, K. (1962). On the nonlinear energy transfer in a gravity wave spectrum. Part I, *J. Fluid Mech.*, 12, 481-500.
16. Huang, N. E. (1986). An estimate of the influence of breaking waves on the dynamics of the upper ocean. *Wave Dynamics*, Ed. O. M. Phillips and K. Hasselmann. 259-314, Plenum Press. New York.
17. Huang, N. E. (1995). Nonlinear Evolution of Water Waves: Hilbert's View, *Proc. 2nd International Symposium on Experimental Chaos* Ed. W. Ditto *et al.*327-341, World Scientific. Singapore.
18. Huang, N. E. And S. R. Long (1980). An experimental study of the surface elevation probability distribution and statistics of wind-generated waves. *J. Fluid Mech.*, 101, 179-200.
19. Huang, N. E., S. R. Long, L. F. Bliven and C. C. Tung (1984). The non-Gaussian joint probability density function of slope and elevation for a nonlinear gravity wave field, *J. Geophys. Res.*, 89, 1961-1972.
20. Huang, N. E., S. R. Long, and L. F. Bliven (1986). An experimental study of the statistical properties of wind-generated gravity waves. In *Wave Dynamics and Radio Probing of the Ocean Surface*, Plenum, New York, pp. 129-144.
21. Huang, N. E., C. C. Tung, and S. R. Long (1990a) Wind-Wave Spectrum , *The Sea*, Vol 9, 197- 238.
22. Huang, N. E. , C. C. Tung, and S. R. Long (1990b). The probability structure of the ocean surface, *The Sea*, Vol 9, 335-366.
23. Huang, N. E., S. R. Long, and Z. Shen (1996). Wave fusion as a mechanism for nonlinear evolution of water waves. *Adv. Appl. Mech.*, Vol. 32, pp. 59-117.

24. Kim, S. K., Liu, P. L-F., and Ligget, J. A. (1983) . Boundary integral equation solutions for solitary wave generation, propagation and run-up. *Coastal Engng.*, 7, 299-317.

25. Komen, G. J., L. Cavaleri, M. Donelan, K. Hasselmann, S. Hasselmann, and P. A. E. M. Janssen (1994). *Dynamics and Modelling of Ocean Waves*. Cambridge U. Press.

26. Lai, R. J., S. R. Long, and N. E. Huang (1989). Laboratory studies of wave-current interaction: Kinematics of the strong interacton, *J. Geophys. Res.*, 94, 16201-16214.

27. Lake, B. M., H. C. Yuen, H. Rundgaldier, and W. E. Ferguson (1977). Nonlinear deep water waves: Theory and experiment. Part 2. Evolution of a continuous wave train. *J. Fluid Mech.*, 83, 49-74.

28. Lake, B. M. and H. C. Yuen (1978). A new model for nonlinear gravity waves. Part 1. Physical model and experimental evidence. *J. Fluid Mech.*, 88, 33-62.

29. Lighthill, M. J. (1965). Contributions to the theory of waves in nonlinear dispersive systems. *J. Inst. Maths. Applics.*, 1, 269-306.

30. Lighthill, M. J. (1967). Some special cases treated by the Whitham theory. *Proc. Roy. Soc. Lond.* A299, 38-53.

31. Long, C. E. and A. H. Salleng (1995). Experiment at Duck, N. C., Beach explores nearshore processes. *EOS Trans.* AGU, 76, 501.

32. Long, S. R. (1992). NASA Wallops Flight Facility Air-Sea Interaction Research Facility, *NASA Ref. Publ.*, RP-1277.

33. Long, S. R., R. J. Lai, N. E. Huang, and G. R. Spedding (1993). Blocking and trapping of waves in a inhomogeneous flow, Dynam. Atmos. Oceans, 20, 79-106.

34. Longuet-Higgins, M. S. and N. D. Smith (1966). An experiment on third order resonant wave interactions. *J. Fluid Mech.*, 25, 417-435.

35. Longuet-Higgins, M. S. (1963). The effect of nonlinearities on statistical distributions in the theory of sea waves. *J. Fluid Mech.*, 17. 459-480.

36. Longuet-Higgins, M. S. (1970a). Longshore currents generated by obliquely incident sea waves, 1. *J. Geophys. Res.*, 75, 6779-6790.

37. Longuet-Higgins, M. S. (1970b). Longshore currents generated by obliquely incident sea waves, 2. *J. Geophys. Res.*, 75, 6779-6790.

38. Longuet-Higgins, M. S. (1982). Parametric solutions for breaking waves. *J. Fluid Mech.*, 121, 403-424.

39. Longuet-Higgins, M. S. (1986). Advances in breaking wave dynamics. In *Wave Dynamics and Radio Probing of the Ocean Surface*, Plenum, New York, pp. 209-230.

40. McGoldrick, L. F., Phillips, O. M., Huang, N., and Hodgson, T. H. (1966). Measurementson resonant wave interactions. *J. Fluid Mech.*, 25, 437-456.

41. McLean, J. W. (1982 a). Instability of finite-amplitude water waves. *J. Fluid Mech.*, 114, 315-330.

42. McLean, J. W. (1982 a). Instabilities of finite-amplitude water waves on water of finite depth. *J. Fluid Mech.*, 114, 331-341.

43. Melville, W. K. (1983). Wave modulation and breakdown. *J. Fluid Mech.*, 128, 489-506.

44. Melville, W. K. and R. J. Rapp (1985). Breaking Waves, *Nature*, 317, 514-516

45. Phillips, O. M. (1960). On the dynamics of unsteady gravity waves of finite amplitude. Part 1. *J. Fluid Mech.*, 9, 193-217.

46. Phillips, O. M. (1967). Theoretical and experimental studies of gravity wave interactions. Proc. Roy. Soc. A, 299, 104-119.

47. Phillips, O. M. (1985). Spectral and statistical properties of the equilibrium range in wind- generated gravity waves. *J. Fluid Mech.*, 158, 505-531.

48. Ramamonjiarisoa, A. and E. Mollo-Christensen (1979). Modulation characteristics of sea surface waves. *J. Geophys. Res.*, 84, 7769-7775.

49. Rapp, R. J. and W. K. Meville (1990). Laboratory measurements of deep water breaking waves. *Phil. Trans. Roy. Soc. Lond.* A 331, 735-780.

50. Spedding, G. R. (1996) 2D complex wavelets for analysis of unsteady, wind-generated surface waves. (In this Issue).

51. Spedding, G. R., F. K. Browand, N. E. Hunag, and S. R. Long (1992). A 2D complex wavelet analysis of an unsteady wind-generated surface wave field. *Dy. Atmos. Ocean*, 20, 55-77.

52. Su, M. Y.(1982 a). Three-dimensional deep-water waves. Part 1, Experimental measurement of skew and symmetric wave patterns. *J. Fluid Mech.*, 124, 73-108.

53. Su, M. Y.(1982 b). Evolution of groups of gravity waves with moderate to high steepness. *Phys. Fluid.*, 25, 2167-2174.

54. Su, M. Y., Bergin, M., Marler, P., and Myrick, R. (1982) Experiments on nonlinear instabilities and evolution of steep gravity wave trains. *J. Fluid Mech.*, 124, 45-72.

55. Su, M. Y., and Green, A. W. (1984). Coupled two- and three-dimensional instabilities of surface gravity waves. *Phys. Fluid.*, 27, 2595-2597.

56. Teng, M. H. and T. Y. Wu (1992). Nonlinear water waves in channels of arbitrary shape. *J. Fluid Mech.*, 242, 211-233.

57. Teng, M. H. and T. Y. Wu (1992). Evolution of long water waves in variable channels. *J. Fluid Mech.*, 266, 207-317.

58. Tuck, E. O. and L. S. Hwang (1972). Long wave generation on a sloping beach. *J. Fluid Mech.*, 51, 449-461.

59. Yuen, H. C. and B. M. Lake (1982). Nonlinear dynamics of deep-water gravity waves. *Adv. Appl. Mech.*, 22, 67-229.

60. Zhang, J. and T. Y. Wu (1996). Personal communication.